Hindawi
Journal of Nanotechnology
Volume 2023, Article ID 6260066, 18 pages
https://doi.org/10.1155/2023/6260066

Research Article

Facile Synthesis and Application of Ag-NPs for Controlling Antibiotic-Resistant*Pseudomonas* spp. and *Bacillus* spp. in a Poultry Farm Environment

Aminur Rahman,[1] Harunur Rasid,[1] Md. Isahak Ali,[1] Nymul Yeachin,[2] Md. Shahin Alam,[3] Khandker Saadat Hossain,[2] and Md. Abdul Kafi [1]

[1]*Department of Microbiology and Hygiene, Bangladesh Agricultural University, Mymensingh 2202, Bangladesh*
[2]*Department of Physics, University of Dhaka, Dhaka 1000, Bangladesh*
[3]*Animal Health Research Division (AHRD), Bangladesh Livestock Research Institute (BLRI), Shavar 1341, Bangladesh*

Correspondence should be addressed to Md. Abdul Kafi; makafi2003@bau.edu.bd

Received 22 December 2022; Revised 2 April 2023; Accepted 8 April 2023; Published 20 April 2023

Academic Editor: Gangaraju Gedda

This study synthesized silver nanoparticles (Ag-NPs) using silver nitrate ($AgNO_3$) as the ion source and sodium tripolyphosphate (STPP) as reducing as well as capping agents. The synthesized Ag-NPs were confirmed initially using Ag-NPs specific λ_{max} at 410 nm with UV-Vis spectrophotometry and homogenously distributed, 100–300 nm size, and round-shaped particles were realized through atomic force microscopy (AFM) and transmission electron microscopy (TEM) image analysis. The various reaction condition-based studies revealed 0.01 M $AgNO_3$ yields maximum particle after 4 h reduction with 1% STPP. *Bacillus* spp. ($n = 23/90$) and *Pseudomonas* spp. ($n = 26/90$) were isolated from three different poultry farms for evaluating the antibacterial activity of Ag-NPs. Among the PCR confirmed isolates, 52% (12/23) *Bacillus* spp. were resistant to ten antibiotics and 65% (17/26) *Pseudomonas* spp. were resistant to eleven antibiotics. The representative resistant isolates were subjected to antibacterial evaluation of synthesized Ag-NPs following the well diffusion method, revealing the maximum sensitive zone of inhibition 19 ± 0.2 mm against *Bacillus* spp. and 17 ± 0.38 mm against *Pseudomonas* spp. The minimum inhibitory concentration (MIC) and minimum bacterial concentration (MBC) of Ag-NPs were 2.1 μg/ml and 8.4 μg/ml, respectively, for broad-spectrum application. Finally, the biocompatibility was determined by observing the viability of Ag-NP-treated BHK-21 cell through trypan blue-based exclusion assay revealing nonsignificant decreased of cell viability ≤2MIC doses. Thus, the synthesized Ag-NPs were proven as biocompatible and sensitive to both Gram-positive and Gram-negative bacteria of the poultry farm environmental samples.

1. Introduction

Antimicrobial resistance (AMR) has emerged as a global health threat because of indiscriminate use of antibiotics in many fields including medical, veterinary medical, and agriculture [1–3]. Nowadays, this threat is increasing proportionately with the increase livestock farming to satisfy huge demand of foods of animal origin [4]. The irrational use of antibiotic and their residues in food chain has been considered as the main cause for such an aggravating situation [5, 6]. Antibiotic resistance often confers to circulate environmental microflora, causing many clinical that are nonresponsive to commercial antibiotics [7, 8]. Therefore, such antibiotic residue laden livestock production does not comply with consumer safety [9]. Generally, commercial farmers are using antibiotics indiscriminately to their farm to obtain maximum production without considering withdrawal periods [10]. As a result, majority of those antibiotics remain as residues in food products that confer antimicrobial resistance to the consumers [11]. The resistance genes are not only confined in the poultry commensal microflora but often confer genes among other environmental microflora [12–14]. This is because human microflora also develop such resistance through plasmid shearing and become resistant to many available antibiotics [15]. If this situation continues, the condition will arise as an emerging catastrophe when bacteria will develop resistance against all the reserve antimicrobials [16]. Considering this, many countries have already forecasted the emergence of post-antibiotic era with serious consequences when a patient would have already died from ordinary septicemia [17]. Thus, AMR has appeared as a potential public health threat in many third world countries where people are prone to bacterial infections [18, 19]. Therefore, exploring new antibacterial for controlling spread of resistance microflora that originated from the poultry farm and poultry farm environments is critically required. Focusing this, many researchers across the globe search for introduction of antibacterial nanomaterials such as chitosan, gold, and silver nanoparticles as an alternate to antibiotics [7].

Ag-NPs possess many unique properties including enhanced functionality, durability of action, surface-to-volume ratio, chemical complexation, increased surface areas, enhanced ion-exchange ability, antitoxicity, and stability [20, 21]. The positively charged surface, ligand replacement ability, and oxidative dissolution capabilities of Ag-NPs facilitate their binding to the negatively charged bacterial cell-wall, resulting in an enhanced bactericidal effect [22, 23]. Because of those advantageous features, Ag-NPs have emphasized in various biomedical [24–26] and biological applications including antibacterial, anticancer [27, 28], anti-inflammatory, antiangiogenic [29], antifungal, antiviral agents [30, 31] and in several other industrial and household applications, such as cosmetic products, medical device coating, freeze coating, optical sensor developments [32], diagnostic device development [33–36], paint industry, food industry, socks, clothing, and disinfectant [37, 38]. Following those applications, recently, many researchers of Bangladesh have already utilized imported nanomaterials from the commercial sources [37]. Likewise, we have also investigated antibacterial activity of commercial Ag-NPs obtained from abroad against poultry pathogens such as *E. coli, Salmonella* spp., and *Staphylococcus* spp. collected from various live bird markets [39]. However, the use of these commercial metal nanoparticles in poultry farming is not feasible because of their high cost, complex engineering, and bioincompatible synthesis [40]. Therefore, easy, cost-effective, and facile nanoparticle synthesis protocol is critically required. Generally, nanomaterial synthesis involves a bottom-up approach (scaling-up of subnano molecules/atoms) using sol-gel process, spray pyrolysis, atomic molecular condensations, vapor depositions, chemicals and electrochemical depositions, and aerosol process [41] and a top-down approach (scaling-down of bulk materials to the nanoscale) using sputtering, thermal or laser ablation, chemical etching, mechanical/ball milling, and explosion processes [42]. All these approaches are not suitable because of low particles yield, limited reproducibility, difficulties in handling, and prolonged reduction time [43, 44]. Moreover, most of the commercially available nanoparticle synthesis methods involved many costly instruments, such as photolithography, nanoimprinting, e-beam lithography, and lyophilizer, for obtaining functional nanomaterials [45, 46]. Such synthesized particles often lost antibacterial performances because of capping agents that irreversibly blocked the functional groups of yielded particles [47]. Overcoming those limitations, the present research was designed for synthesizing Ag-NPs using a facile sol-gel method avoiding the use of any capping agent for obtaining nanoparticles with maximum antibacterial activity.

Herein, a facile sol-gel, bottom-up synthesis approach was employed for attaining high volume with homogenously disperse antimicrobial nanoparticles [48–50]. For this, the proposed method employed $AgNO_3$ as the ion source, sodium tripolyphosphate (STPP) as reducing agents and capping/stabilizing agents [51]. The synthesized Ag-NPs were confirmed using UV-Vis spectrophotometry and atomic force microscopy (AFM). For the antibacterial evaluation and stability of Ag-NPs, antibiotic resistance *Bacillus* spp. (as a candidate of Gram-positive) and *Pseudomonas* spp. (as a candidate of Gram-negative bacteria) were isolated from the different poultry environments surrounding the Bangladesh Agricultural University campus. The minimum inhibitory concentration (MIC) and minimum bacterial concentration (MBC) were determined following broth dilution and the agar diffusion method [52, 53]. The antibacterial effect of synthesized Ag-NPs against isolated bacteria was evaluated through standard dish diffusion methods followed by measuring the zone of inhibition in comparison with resistance antibiotic of cephalexin and chloramphenicol [54, 55]. Recently, antimicrobial residue in poultry and poultry products is considered as a potential contributor of emergence of resistant microflora in the environment [56]. The rapid expansion of poultry industry aggravated this situation and became a serious public health threat because of irrational use of antibiotics and antibiotic residue laden poultry [57, 58]. Overcoming this situation, many researchers also synthesized antimicrobial nanomaterials as an alternative of commercial antibiotics [59–64]. However, these antibacterial nanomaterials are not suitable for *in vivo* application due to their bioincompatible nature [59, 65–67]. So, the biocompatible antibacterial nanomaterial is critically required prior to *in vivo* applications. Hence, this research focused on synthesis and characterization Ag-NPs as antimicrobial nanomaterials against bacteria isolated from poultry and cytotoxicity effect evaluation using BHK-21 cell line following trypan blue exclusion assay. The Ag-NP synthesis program employed a simple cost-effective sol-gel method for ensuring maximum particle yield, enhancing antibacterial activity [68, 69]. Thus, the synthesized biocompatible antibacterial Ag-NPs could be employed as an alternative of antibiotics for tackling resistance bacterial infection in the poultry farms and thereby impact on curving the use of antibiotics in poultry farming.

2. Materials and Methods

The approached methodologies of the study include three major tasks, namely, (i) facile synthesis of Ag-NPs, (ii) isolation and identification of bacteria, and (iii) antibacterial effect evaluation of the yielded nanoparticles. The facile synthesis protocol was realized through several trial experiments for determining appropriate concentration of ion source and optimum reduction periods. The antibacterial activity assay was performed by the standard dish diffusion method [70] using the synthesized Ag-NPs against the bacteria isolated from various environmental settings surrounding poultry farms. The antibacterial sensitivity and stability of Ag-NPs were determined by measuring the diameter of zones of inhibition surrounding the wells [42, 46]. The minimum inhibitory concentration (MIC) and minimum bacterial concentration (MBC) of yielded Ag-NPs were also determined using UV-Vis spectroscopy following the broth dilution and Agar dilution methods [71].

2.1. Materials. Silver nitrate ($AgNO_3$) and sodium tripolyphosphate (STPP) were purchased from Sigma Aldrich, USA. Bacterial culture medium (nutrient broth, nutrient agar, Tryptic Soy Agar, blood agar, Mueller–Hinton Agar, and Mueller–Hinton Broth) were purchased from HiMedia Laboratories Pvt. Ltd., Mumbai, India. PCR master mixer, primer sets (16s rRNA gene and 16s rDNA gene), agarose powder, DNA ladder, Tris-acetate-EDTA (TAE) buffer, and nuclease free water were purchased from Promegra, Madison, USA. All the materials were received in purish grade and used as instructed in the safety datasheet.

2.2. Synthesis of Silver Nanoparticles (Ag-NPs). For synthesis of Ag-NPs, 0.05 M STPP solution was prepared as reducing agents and 0.1 M, 0.01 M, and 0.001 M $AgNO_3$ solutions were prepared as ion source according to the methods by Wang et al. and Zielińska et al. [38, 72] as illustrated in Figure 1. The freshly prepared STPP solution was added into different concentrations of $AgNO_3$ solution (0.1 M, 0.01 M, and 0.001 M) at ratio 1 : 5 and stirred at various periods (1–5 h) for 1200 rpm at 80°C until the color changed. The solution color was monitored and a small amount of Ag-NPs solution was collected in every hour interval. When the golden color solution was achieved, all the collected solution was characterized and the suitable reduction reaction period was confirmed. After confirming suitable reduction time, the Ag-NPs were further synthesized on $AgNO_3$ concentration basis (0.1 M, 0.01 M, and 0.001 M) for obtaining maximum Ag-NPs solution. Once the solution color shifted from transparent to golden color, all the mixtures were centrifuged at 1300 rpm for 10 minutes, and the supernatant was collected for physical characterization and antibacterial effect evaluation.

2.3. Physical Characterizations of Ag-NPs. The morphological features of synthesized Ag-NPs were investigated with atomic force microscopy (AFM, Nano surf Flex) using contact mode to determine the particle size and dimension [73]. Before taking images, the supernatant was spin-coated at 1300 rpm and dried in an oven at 60°C. The measurement was performed in a faradic case at room temperature. The dimensions of the nanostructures were measured from the height profile of topographic images. Whereas, the physical structural morphology of yielded Ag-NPs was determined through transmission electron microscopy. The concentration of Ag-NPs was investigated with UV visible spectra recorded with a UV-Vis spectrometer [74] at the range 300 nm–500 nm for confirming the concentration of synthesized nanoparticles where distilled water was kept as a control. Data obtained from blank solution and chemically synthesized Ag-NPs solution were compared viewing the shifting of the bandgap.

2.4. Isolation and Identification of Bacteria from Poultry Farm Environment

2.4.1. Sample Collection and Morphological Characterization. The air, drainage, and surface swab samples ($n = 90$) of poultry farm were collected from different poultry farms (such as Al-hira farm, Trisal, BAU Poultry farm, and Shahidul farm, Modhupur) surrounding Bangladesh Agricultural University, Mymensingh, Bangladesh. The drainage and surface samples were collected and incubated into a shaker incubator at 37°C overnight utilizing nutrient broth for enrichment of the culture. The enriched culture was streaked on a nutrient agar medium and incubated at 37°C for 24 h. The air sample was collected by exposing the nutrient agar plate inside and outside of the farm for 30 minutes and transferred into the incubator through ice box aseptically [75]. The fresh single colony from the incubated nutrient agar medium plate was picked and again streaked to a bacteria-specific medium such as MacConkey agar medium and blood agar medium and incubated at 37°C for 24 h for investigating cultural characteristics of specific bacteria. Then, the pure colony from the specific culture medium was subcultured and a pure single colony from the selective medium was smeared on a sterilized glass slide and air-dried. The dried slide was heat fixed and stained with gram-staining materials following standard operating procedure [76].

2.4.2. Biochemical Confirmation. For further confirmation of bacteria, the five basic sugars (dextrose, maltose, mannitol, glucose, and sucrose) fermentation test was performed. 100 μl of pure broth culture of the isolated bacteria was inoculated into a broth containing dextrose, maltose, mannitol, glucose, and sucrose and incubated at 37°C for 18 h. Finally, observed sugar fermentation and/with gas formation in the inoculated test tube for biochemical confirmation of isolated bacteria [77].

2.4.3. Confirmation of Genus Specific Genes Using PCR. DNA extraction of *Bacillus* spp. and *Pseudomonas* spp. was performed following boiling method according to the method by Al-Hejjaj et al. [78]. For polymeric chain reaction (PCR), the master mixture (25 μl) was prepared according to the method by Mohamed et al. [79] where the thermal profiles of *16s rRNA* gene for *Bacillus* spp. and *16s rDNA*

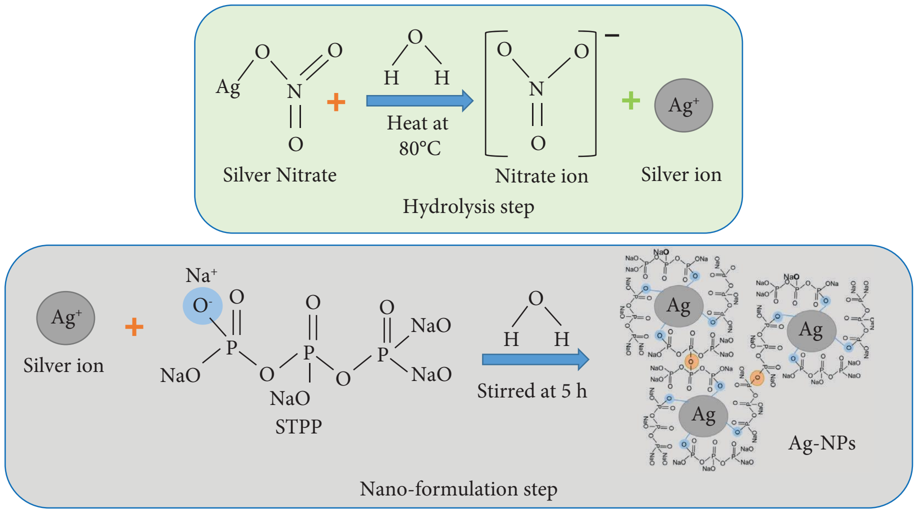

Figure 1: Schematic illustration of the Ag-NPs synthesis process.

gene for *Pseudomonas* spp. (Table 1). For preparing 1.5% agarose gel, 0.45 g of nobel agar was dissolved into 1 X TAE buffer. After solidification, the gel was transferred to the electrophoresis tank and loaded with 3 μl of loading dye (range 100–1000 bp), 5 μl of amplified PCR product, and a control in the wells. The leads of the electrophoresis apparatus were connected to the power supply and electrophoresis was run at 100 V for 25 minutes. The gel was stained in ethidium bromide (0.5 μl) for 10 minutes in a dark place. Then, the gel was destained in distilled water for 2 minutes and then transferred to UV transilluminator in the dark chamber for optical documentation.

2.5. Determination of Antibiotic Resistance Pattern of Bacillus spp. and Pseudomonas spp. The PCR confirmed *Bacillus* spp. and *Pseudomonas* spp. were subjected to the determination of antibiotic resistance pattern, following antibiogram profiling using commercially available antibiotics discs. The antibiotic resistance patterns against of those isolates were determined by measuring the zone of inhibitions surrounding the discs following disc diffusion methods (Bauer et al., 1966).

2.6. Determination of Antibacterial Activity and Stability of Ag-NPs. The antibacterial activities and stability of Ag-NPs were determined following the dish diffusion method [70]. The single colony of isolated bacteria (*Bacillus* spp. and *Pseudomonas* spp.) was inoculated into nutrient agar and incubated overnight. The freshly cultured broth was employed for preparing 0.5 McFarland (10^5 cfu/ml) bacterial culture according to Clinical and Laboratory Standards Institute [82]. After incubation, 100 μl of each bacterial samples were spread on freshly prepared Mueller–Hinton agar and each MH agar plate, 5 wells in a diameter of 3 mm were cut and 50 μl of Ag-NPs were placed in three wells, and cephalexin and chloramphenicol were placed in each well for *Bacillus* spp. and *Pseudomonas* spp., while control was kept empty for each plate. The MH plate incubated overnight for measuring zones of inhibition [83]. Likewise, the stability of yielded particles was tested using the stability of UV-Vis spectroscopic λ_{max} peak, and measuring the zones of inhibition of Ag-NPs appeared during antibacterial activity assay. The experiment was replicated thrice, and the zones of inhibition were measured using slide calipash. Data obtained from inhibitory zones were used for categorizing levels of sensitivity/resistance according to CLSI 2019.

2.7. Minimum Inhibitory Concentration (MIC) and Minimum Bacterial Concentration (MBC) Determination. The MIC of yielded Ag-NPs was measured using UV-Vis spectroscopy following the broth dilution methods as shown in Figure 2 [84]. The 2-fold dilution (Figure 2(a)) of differently synthesized Ag-NPs was prepared sequentially with freshly prepared Mueller–Hinton broth. Then, 100 μl of the 0.5 McFarland (10^5 cfu/mL) bacterial culture (*Bacillus* spp. and *Pseudomonas* spp.) were added into each dilution without control and incubated at 37°C for 24 h. The turbidity of each incubated tube was measured optically and UV-Vis spectroscopically (Figure 2(b)) compared with control turbidity [85]. The maximum percentages (100–95%) of transparency with an inhibited bacterial growth were considered as MIC [86]. Additionally, the MBC of each dilution was measured following the Agar dilution method (Figures 2(c) and 2(d)), using 100 μl of dilutions of MIC without visible turbidity and incubated at 37°C for 24 h. Finally, the lowest concentration at which the bacteria did not grow was considered as MBC.

2.8. Determination of Biocompatibility of Ag-NPs

2.8.1. Cell Culture and Maintenance. The cytotoxic effect of Ag-NPs was determined using BHK-21 cell line. For this, a frozen cell was thawed and seeded in the cell culture plates providing all necessary nutrients such as DMEM supplemented with 1% pens-step and 10% FBS and incubated aseptically at 37°C with 70% humidity and 5% CO_2 for achieving monolayer culture. The confluent cells from the

Table 1: Thermal profile for amplification of the used bacteria.

Name of the bacteria	Target gene	Thermal profile	Amplicon size (bp)	Reference
Bacillus spp.	*16s rRNA gene*	Initial denaturation at 94°C for 5 minutes, followed by 30 cycles of denaturation at 95°C for 30 seconds, annealing at 55°C for 20 seconds, and extension at 72°C for 30 seconds. The final extension was conducted at 72°C for 7 minutes	463	[80]
Pseudomonas spp.	*16s rDNA gene*	Initial denaturation at 95°C for 2 minutes, followed by 25 cycles of denaturation at 94°C for 20 seconds, annealing at 54°C for 20 seconds, and extension at 72°C for 40 seconds. The final extension was conducted at 72°C for 1 minute	618	[81]

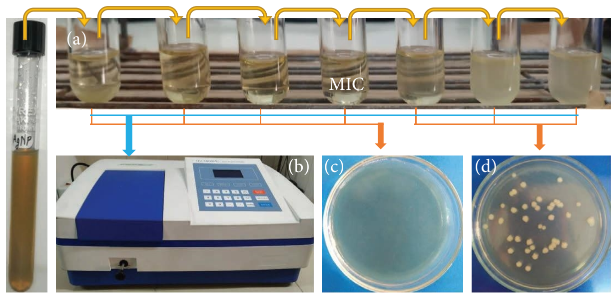

Figure 2: Determination of MIC according to CLSI 2019 where (a) two-fold serial dilution of Ag-NPs, (b) measurement of turbidity using UV-Vis spectroscopy (UV-1600PC), (c) inhibition of bacterial growth on MH agar, and (d) bacteria growth on MH agar.

third passages were utilized for the determination of Ag-NPs treated cell viability following trypan blue exclusion assay [87, 88].

2.8.2. Cell Viability Assay. For the detection of cytotoxic effect of Ag-NPs, different doses of Ag-NPs were treated into confluent monolayer of BHK-21 cell and their viabilities were calculated according to the method by Kamiloglu et al. [89]. For calculating cell number, 10 μl of trypan blue was mixed with cell suspension and applied to a hemocytometer. The hemocytometer was investigated under a microscope for counting all 4 sets of 16 corners, while the stained cells were excluded from counting.

2.9. Statistical Analysis. Data obtained from the thrice replication on the inhibitory effects from the differently prepared chitosan nanoparticle solution were analyzed with one-way ANOVA followed by paired t-test performed for standard error and the P value. The level of significance was determined using the Bonferroni posthoc test where $^{*}P$ values <0.05 were considered the significance level.

3. Results

3.1. Synthesis and Physical Characterization of Ag-NPs

3.1.1. Synthesis of Ag-NPs. The Ag-NPs synthesis programme employed $AgNO_3$ as Ag^+ ion source and sodium tripolyphosphate (STPP) as a reducing as well as capping agent. Such chemical synthesis was initially confirmed by observing color shifting from transparent to golden solution during the reduction reaction period (Figure 3). The result revealed that golden color Ag-NPs solution was obtained at 4 h reduction period whereas, almond color was obtained at 3 h and cider orange color was achieved after 5 h reduction as shown in Figure 3(a). The solution color was transparent and brown at 1 h and 2 h reaction, respectively, as shown in Figure 3(a). Such shift in color was due to the variation of particle yields with various reduction reaction periods. These particles concentration-based shift in color was further investigated quantitatively using Ag-NP specific λ_{max} at 410 nm obtained from UV-Vis spectroscopy. The UV-Vis spectra showed maximum particle yielded at 4 h reduction reaction as indicated in green line of Figure 3(b), whereas at 1 h, 2 h, and 3 h reduction reaction, the particle yield was increased gradually as indicated in black, red, and blue line of Figure 3(b). In case of 5 h reduction, the particles yield decreased as indicated in violet line of Figure 3(b). Considering the maximum particle yield, the 4 h reduction reaction was selected for further Ag-NPs synthesis with varying $AgNO_3$ concentration to determine optimum concentration of ion source.

The absorbance spectrum of yielded Ag-NPs from various concentrations of $AgNO_3$ solution is presented in Figure 4, where inset showed golden color with maximum Ag-NPs achieved when 0.01 M $AgNO_3$ was employed whereas, squirrel and cider orange color with minimum Ag-NPs achieved when 0.1 M and 0.001 M $AgNO_3$ was employed. The corresponding UV-Vis spectroscopy revealed that, maximum Ag-NPs yielded at concentration of 0.01 M as indicated in red line whereas, relatively less Ag-NPs yielded at the concentration of 0.1 M and 0.001 M, respectively, as indicated in black and blue line of Figure 4. Such variations of particle yield were resulted from the variations of ration between ion source and reducing agent. However, the synthesized Ag-NPs were further confirmed by physical characterization using AFM.

3.1.2. Morphological Investigation with AFM and TEM. Three-dimensional (3D) topographic AFM images were analyzed to determine morphology and dimensions of yielded Ag-NPs as shown in Figure 5. The results revealed that, the maximum nanoparticles with homogenous dimension were achieved when 0.01 M $AgNO_3$ solution employed as shown in Figure 5(c). Whereas, non-homogenous dimensions of Ag-NPs was noticed from 0.1 M to 0.001 M $AgNO_3$ solution as shown in Figures 5(b) and 5(d), while no such particle was observed from the control surface as shown in Figure 5(a).

The TEM images were employed for realizing the actual morphological features of the yielded particles. The TEM image of yielded Ag-NPs revealed a round-shaped particle with 100–300 nm size nanoparticles was obtained when 0.01 M $AgNO_3$ solution was employed as the ion source as shown in Figure 6(b). Whereas, no such particle yield was observed from the control surface as shown in Figure 6(a).

3.2. Isolation and Identification of Bacteria. Among the 90 (ninety) poultry farm, environmental samples 23 (twenty-three) were characterized as *Bacillus* spp. and 26 (twenty-three) as *Pseudomonas* spp. Here, the colony morphology of isolated bacteria was used for determining the bacteria as shown in Figure 7. The large, flat, granular to ground grass, and β-hemolytic colonies on blood agar medium indicates *Bacillus* spp. as shown in Figure 7(a). Whereas, circular, smooth, raised, and blue-green colonies on MacConkey agar media indicating *Pseudomonas* spp. as shown in Figure 7(d). The Gram's staining of a single colony from blood agar medium smeared on a freshly cleaned glass slide showed rod-shaped ones with square-ended purple color indicating Gram-positive *Bacillus* spp. as shown in Figure 7(b).

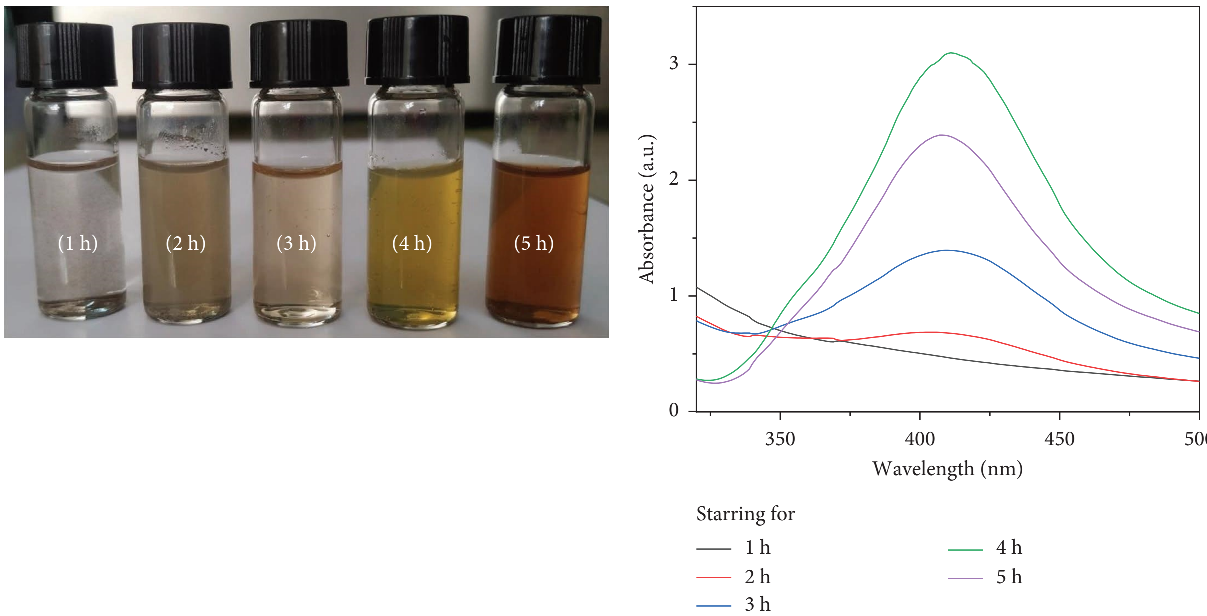

(a) (b)

Figure 3: Color shift of synthesized Ag-NPs at different reduction time: (a) at 1–5 h and (b) the corresponding UV-Vis data.

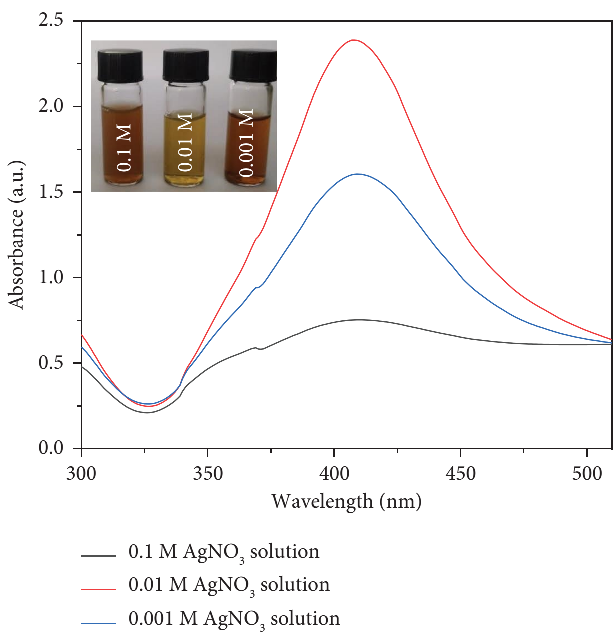

Figure 4: Determination of maximum Ag-NPs yielding potentiality employing different concentrations of ion source ($AgNO_3$) using UV-Vis spectroscopy and their color shifting.

Whereas, small rod with pink color bacterium from the smeared prepared with a single colonies from MacConkey agar indicated Gram-negative*Pseudomonas* spp. as shown in Figure 7(e). The sugar fermentation test revealed color changes along with gas formation in dextrose, and for *Bacillus* spp. (see Figure S1a) while, no color change and gas formation occurred in dextrose, maltose, lactose, and sucrose except mannitol for *Pseudomonas* spp. (see Figure S1b).

The amplified PCR product using primer of *16s rRNA* gene showed 463 bp band size when DNA extracted from blood agar was employed. The PCR product band at 463 bp indicated *Bacillus* spp. as shown in Figure 7(c). Whereas, amplified PCR product using primer of *16s rDNA* gene showed 618 bp band size when DNA extracted from MacConkey agar was employed indicating *Pseudomonas* spp. as shown in Figure 7(f).

3.3. *Determination of Antibiotic Resistance Pattern of Bacillus spp. and Pseudomonas spp. Using Commercial Antibiotics.*

The antibiotic resistance pattern against those isolates was determined by measuring the zone of inhibitions surrounding the disc as shown in Figure 8. Among all isolated *Bacillus* spp., 52% (12/23) isolates showed resistant (8 ± 0.7 mm zone of inhibition) to ten antibiotics, namely, aztreonam, ampicillin, cefixine, vancomycin, doxycycline, linezolid, erythromycin, trimethoprim, levofloxacin, and moxifloxacin out of 12 antibiotic tested as shown in Figure 8(a). While, gentamycin and chloramphenicol showed sensitive (15 ± 0.7 mm) zone of inhibition according to CLSI 2019. However, in case of *Pseudomonas* spp., 65% (17/26) isolates showed resistant (9 ± 0.6 mm) to eleven antibiotics, namely, ampicillin, cefixime, aztreonam, vancomycin, doxycycline, linezolid, erythromycin, chloramphenicol, trimethoprim, levofloxacin, and moxifloxacin, while only gentamycin (17 ± 0.6 mm) showed sensitivity to all isolates as shown in Figure 8(b). Thus, the antibiotic resistant *Bacillus* spp. and *Pseudomonas* spp. were subjected to antibacterial activity evaluation of yielded Ag-NPs.

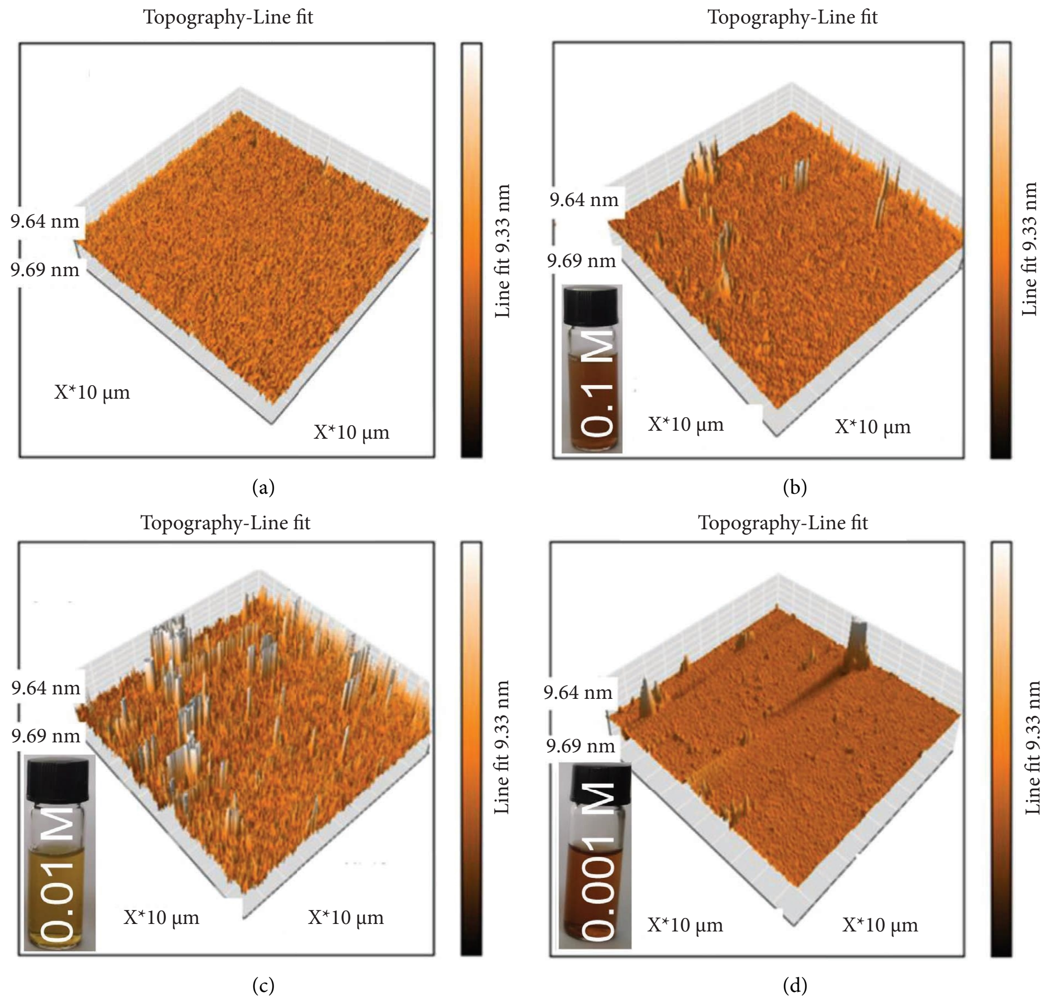

Figure 5: AFM images of various concentrations of $AgNO_3$-based synthesized Ag-NPs: (a) control surface, (b) 0.1 M, (c) 0.01 M, and (d) 0.001 M.

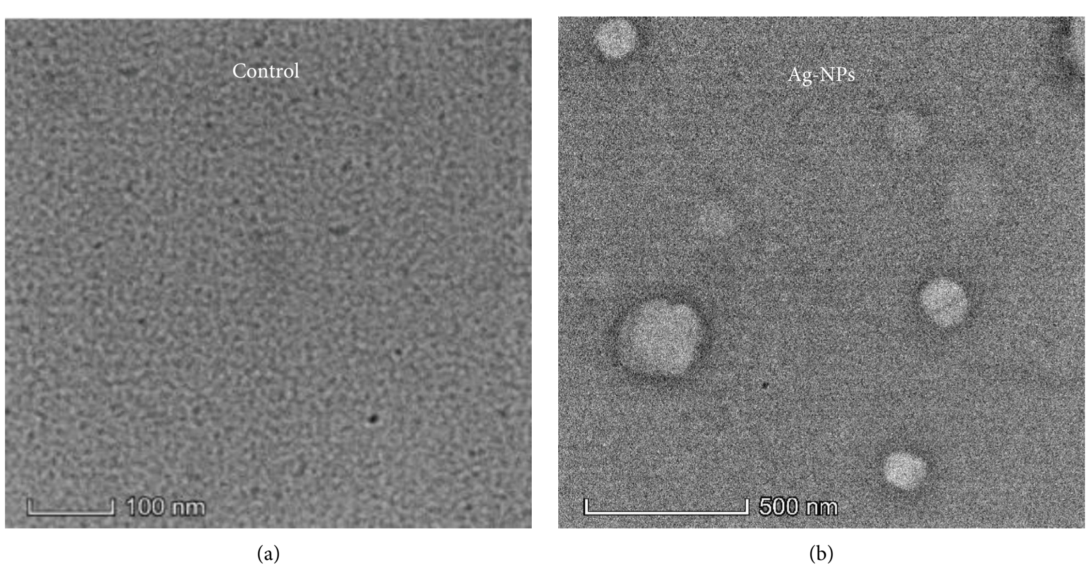

Figure 6: The TEM images of yielded Ag-NPs: (a) control surface and (b) Ag-NPs coated surface.

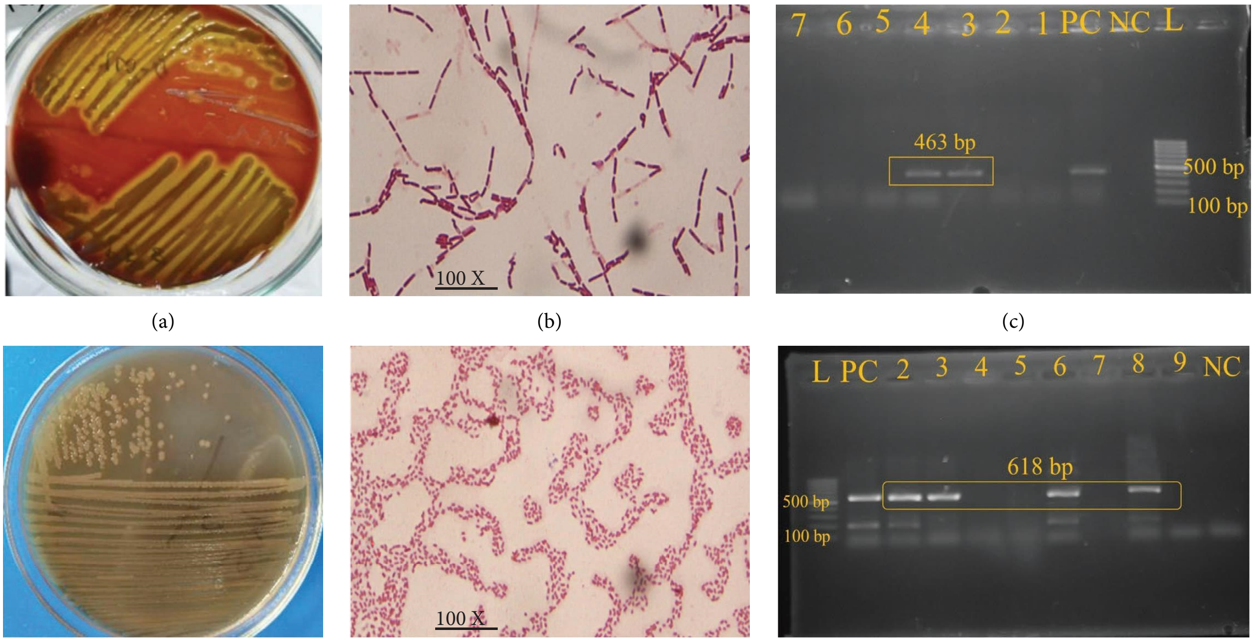

(a) (b) (c)

(d) (e) (f)

Figure 7: Isolation and identification of (a), (b), and (c) morphological, Gram's staining, and molecular detection of *Bacillus* spp. and (d), (e), and (f) morphological, Gram's staining, and molecular detection of *Pseudomonas* spp.

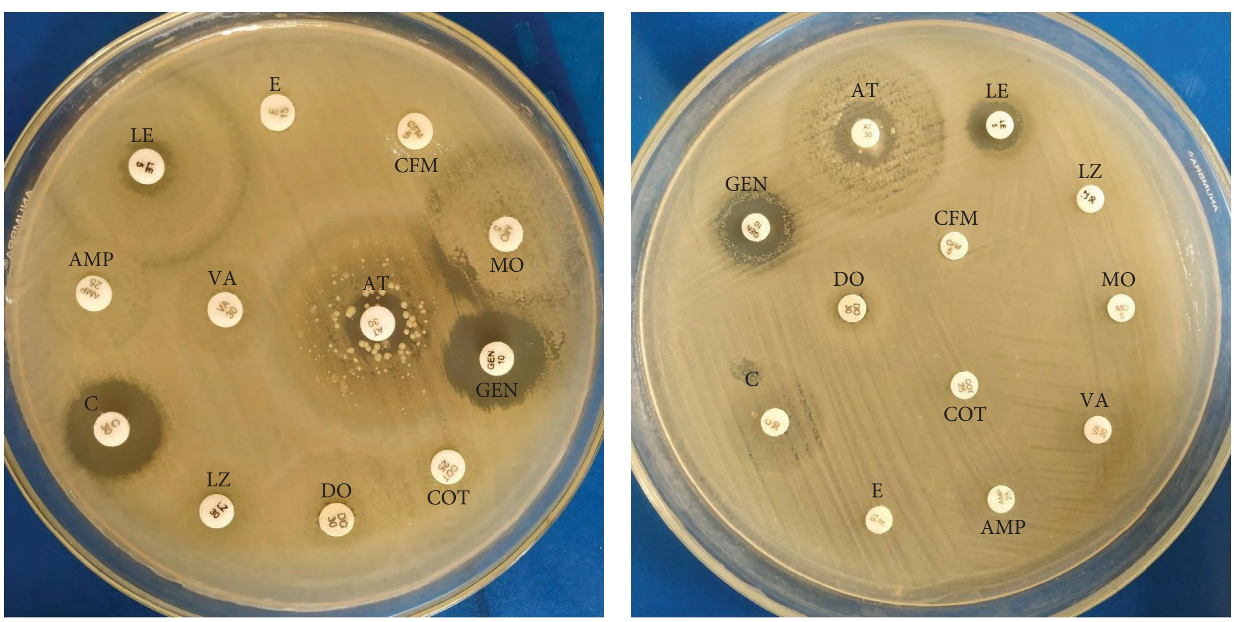

(a) (b)

Figure 8: Antibiogram profile using 12 antibiotics (E: erythromycin, CFM: cefixime, OM: moxifloxacin, GEN: gentamycin, COT: trimethoprim, DO: doxycycline, LZ: linezolid, C: chloramphenicol, AMP: ampicillin, LE: levofloxacin, VA: vancomycin, and AT: aztreonam) covering several class against (a) *Bacillus* spp. and (b) *Pseudomonas* spp.

3.4. Determination of Antibacterial Activity of Synthesized Ag-NPs. The confirmed antibiotic resistance isolates (*Bacillus* spp. and *pseudomonas* spp.) from poultry environment were subjected to antibacterial evaluation of the yielded nanoparticle. The antibacterial effect of synthesized Ag-NPs utilizing different $AgNO_3$ concentrations were determined by measuring the zone of inhibitions as shown in Figure 9. The results revealed that maximum zoon of inhibition of Ag-NPs (19 ± 0.4 mm) against *Bacillus* spp. was observed when Ag-NPs synthesized utilizing 0.01 M $AgNO_3$ solution, and minimum zoon of inhibition of Ag-NPs (11 ± 0.2 mm) was observed when Ag-NPs synthesized utilizing 0.1 M $AgNO_3$

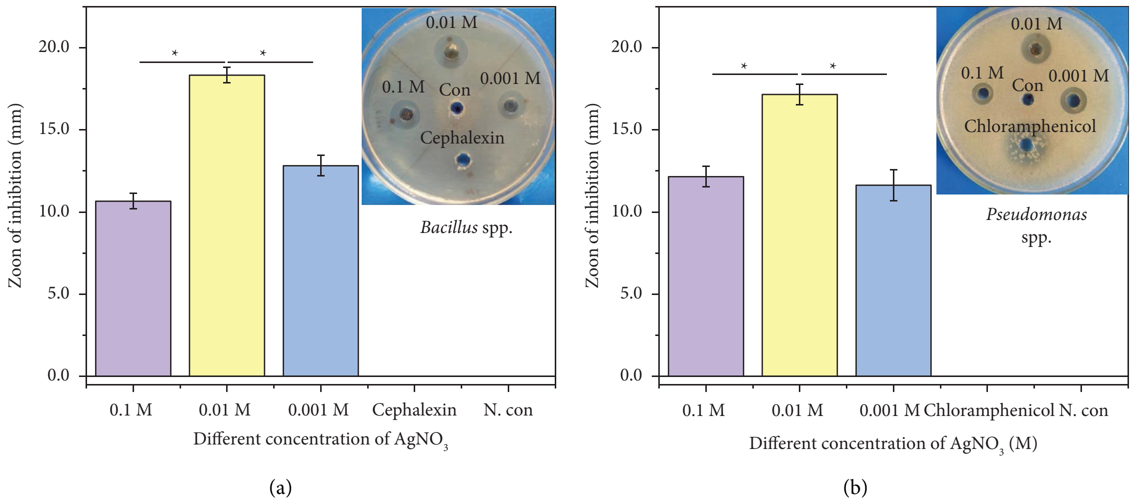

Figure 9: Images showing zone of inhibition of Ag-NPs in comparison with resistance antibiotics: (a) *Bacillus* spp. and (b) *Pseudomonas* spp. (*remarked the significant level of zone of inhibition).

solution as shown in Figure 9(a). Likewise, maximum zoon of inhibition of Ag-NP (17 ± 0.38 mm) against *pseudomonas* spp. was observed when Ag-NPs synthesized utilizing 0.01 M $AgNO_3$ solution, and minimum zoon of inhibition of Ag-NPs (12 ± 0.3 mm) was observed when Ag-NPs synthesized utilizing 0.1 M $AgNO_3$ solution as shown in Figure 9(b). While, cephalexin and chloramphenicol and negative control showed no zone of inhibition against *Bacillus* spp. and *Pseudomonas* spp. Thus, *Bacillus* spp. and *Pseudomonas* spp. were considered as resistant bacteria to antibiotic, but susceptible to the synthesized Ag-NPs.

3.5. Stability of Synthesized Ag-NPs. The stability of particle size and their antibacterial activity were determined at different periods of post synthesis using UV-Vis spectroscopy and antibacterial activity assay. The absorbance peaks λ_{max} at 410 nm of Ag-NPs were stable till 5^{th} day post synthesis, whereas the absorbance peak was shifted from 410 nm to 420 nm with decreasing peak intensity at 6^{th} day post synthesis was noticed as shown in Figure 10(a). Likewise, in case of antibacterial effect assay, the zones of inhibition surrounding the Ag-NPs treated well were observed till 5^{th} day post synthesis, while the zone of inhibition was significantly decreased at the 6^{th} day post synthesis as shown in Figures 10(b) and 10(c). Thus, both the study confirmed the particles in yielded solution were stable till 5^{th} day post synthesis. However, lyophilization of the yielded particle will prolong the stability of particle.

3.6. Minimum Inhibitory Concentration (MIC) and Minimum Bacterial Concentration Determination (MBC). After 24 h of incubation at 37°C, transmittance (%) for all Ag-NPs diluted test tubes were measured using UV-Vis spectroscopy for MIC and MBC determination as shown in Figure 11. The result revealed that, in case of Gram-positive bacteria of *Bacillus* spp. MIC was 1.06 μg/ml (showed 98–100% transparency) at the dilution of 10^{-5} when Ag-NPs were synthesized utilizing 0.01 M $AgNO_3$ solution as shown in Figure 11(a). Whereas, turbidity with huge bacterial growth (showed 20–25% transparency) was observed at the same dilution (10^{-5}) when Ag-NPs synthesized with 0.1 M and 0.001 M $AgNO_3$ solution. Likewise, in case of Gram-negative bacteria of *Pseudomonas* spp. MIC was 4.2 μg/ml (showed 100–97% transparency) at the dilution of 10^{-3} when Ag-NPs were synthesized utilizing 0.01 M $AgNO_3$ solution as shown in Figure 11(b). Whereas, turbidity with huge bacterial growth (showed 10% transparency) was found at the same dilution when Ag-NPs synthesized utilizing 0.1 M and 0.001 M $AgNO_3$ solution. At the same time, the MBCs of Ag-NPs for *Bacillus* spp. was 2.1 μg/ml when Ag-NPs synthesized utilizing 0.01 M $AgNO_3$ solution. Whereas, the MBCs of Ag-NPs for *Pseudomonas* spp. was 8.5 μg/ml when Ag-NPs synthesized utilizing 0.01 M $AgNO_3$ solution. Thus, this study suggested 0.213 mg/ml Ag-NPs and 0.426 mg/ml of Ag-NPs as broad spectrum of MIC and MBC dose, respectively.

3.7. Cell Viability for Cytotoxicity Evaluation of Ag-NPs. For biosafety evaluation, different MIC doses of Ag-NPs treated BHK-21 cell viability was determined by trypan blue exclusion assay. The cell viability of the Ag-NPs treated BHK-21 cell showed nonsignificant difference $(0.29) \leq 2$ MIC. Whereas, a significant difference (0.0000006) of cell viability was noticed from cell treated with 3 MIC doses compared with control cell as shown in Figure 12.

4. Discussion

This nanoparticle synthesis program employed $AgNO_3$ as primary Ag^+ ion source and sodium tripolyphosphate (STPP) as reducing as well as capping agent [90]. Various periods of reduction reaction dependent synthesized Ag-NPs were initially confirmed by observing color shift from transparent to golden [91]. The maximum golden color solution at 4 h reduction period was resulted from the

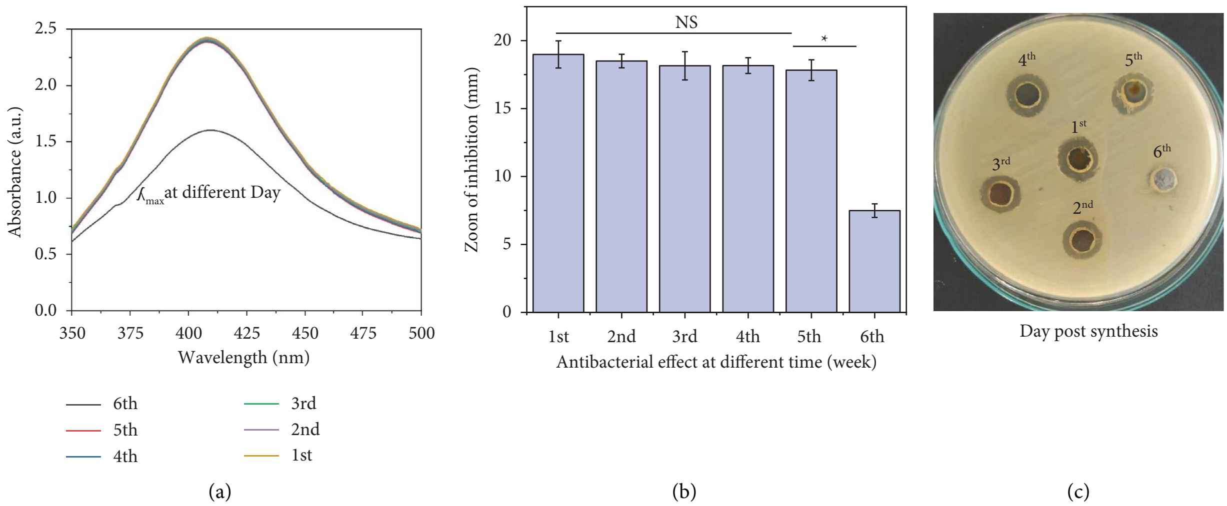

Figure 10: Stability test of synthesized Ag-NPs: (a) absorbance peak (λ_{max}) at 410 nm, (b) inhibitory zone diameter, and (c) image showing zone of inhibition surrounding Ag-NPs treated well.

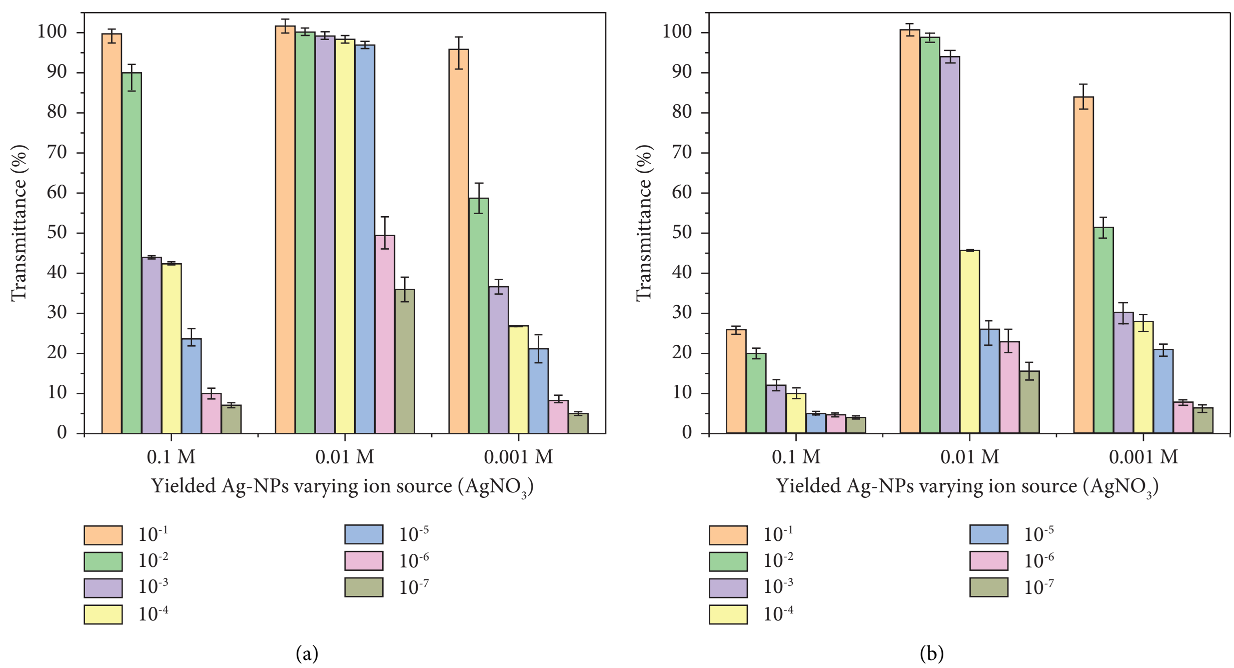

Figure 11: Measurement of transmittance (%) for determination of the minimum inhibitory concentration of Ag-NPs on turbidity based using UV-Vis spectroscopy for (a) *Bacillus* spp. and (b) *Pseudomonas* spp.

complete reduction of Ag^+ ion [92]. Whereas, almond color solution was obtained at 3 h because of an incomplete reduction reaction [93, 94]. Cider orange color solution at 5 h reduction reaction resulted due to the aggregation of synthesized particle due to prolong exposure of the reducing agent [95]. In case of 1 h and 2 h reduction reaction, transparent and brown color solutions were appeared due to insufficient reduction reaction. This optical observation was further verified using UV-Vis spectroscopic analysis using the Ag-NPs specific absorption peak (λ_{max}) 410 nm [96]. It is well known that nanoparticle induces specific surface plasmon resonance depending of type of material and particle size [97, 98]. Thus absorption peak (λ_{max}) at approximately between 400–410 nm wave length was employed for confirming the Ag-NPs synthesis [68, 99]. This Ag-NPs synthesis was initiated with the hydrolysis of $AgNO_3$ salt into Ag^+ and NO_3^- ions [100]. Later, this Ag^+ ion was reduced to form Ag^0 using STPP. For that, STPP was dissolved by heating at 80°C to form $P_3O_{10}^{5-}$ and Na^{5+} ions in the solution [101, 102]. This $P_3O_{10}^{5-}$ employed for the reduction of Ag^+ ion to form Ag°, and finally several Ag° were aggregated during reduction reaction for the formation of Ag-NPs [103]. Thus, the size of the nanoscale particles was achieved through adjusting the concentrations of ion source,

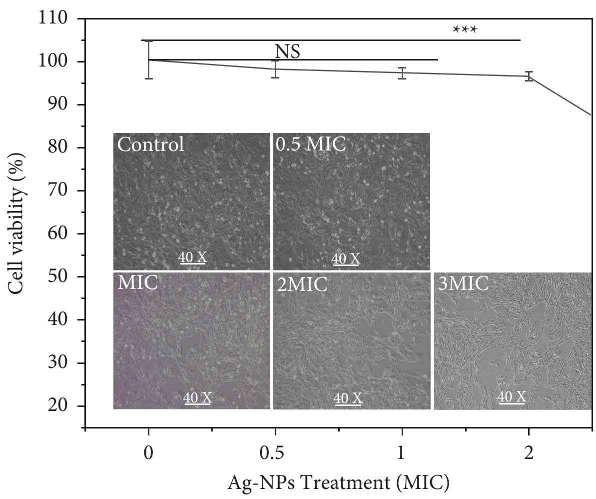

Figure 12: Determination of cell viability of Ag-NPs treated BHK-21 cell using trypan blue exclusion assay.

reducing agents, and period of reduction [104, 105]. The maximum absorption peak at 410 nm confirmed that highest Ag-NPs were yielded at 4 h reduction reaction. Whereas, relatively less intense absorption peak at 405 nm indicated low Ag-NPs yield at 1 h, 2 h, and 3 h reduction reaction. Many previous studies showed such absorption peak intensity based varying concentration of particle yield elsewhere [99, 106, 107]. In case of 5 h reduction period, less intensity of absorption peak at 400 nm indicates the threshold of the reduction reaction period for optimum Ag-NPs yield [108]. Thus, 4 h reduction reaction time was selected for further Ag-NPs synthesis with varying $AgNO_3$ concentration to determine optimum concentration of ion source.

Suitable concentrations of ion source for Ag-NPs synthesis was confirmed with golden color solution after complete reduction reaction. The golden color indicated the maximum Ag-NPs yield when 0.01 M $AgNO_3$ was employed [91, 92, 109]. Whereas, squirrel and cider orange color with minimum Ag-NPs was yielded when 0.1 M and 0.00 1 M $AgNO_3$ solution was utilized. The highest absorption peak (λ_{max}) at 405 nm confirmed that maximum Ag-NPs were yielded at concentration of 0.01 M because of the appropriate ration of ion source and reducing agent [110]. Whereas, relatively less intensity of the absorption peak at 405 nm confirmed that relatively less Ag-NPs were yielded at a concentration of 0.1 M and 0.001 M due to presence of inappropriate ratio of ion source and reducing agent. Such concentration of ion source and reducing agent based varying particle yields were reported for many other nanoparticles elsewhere [21, 38, 72, 96]. These visual and spectroscopic observations were further verified with various physical characterization tools for realizing morphological features of the yielded particles [111–117]. The three-dimensional topographic atomic force microscopic images showed that, the maximum nano particles with homogenous dimension were obtained when 0.01 M $AgNO_3$ solution was employed. Whereas, nonhomogenous dispersed Ag-NPs observed when 0.1 M and 0.001 M $AgNO_3$ solution were employed. While, no such particle was noticed from control surface. Such AFM observations completely coincided with UV-Vis spectroscopic analysis. The TEM analysis also revealed round to spherical shaped (100–300 nm) nanoparticles yielded from 0.001 M ion source with 15% reducing agent at 4 h reduction indicating formation of Ag-NPs.

The physically confirmed Ag-NPs were subjected to antibacterial evaluation against bacteria isolated from various environmental settings of poultry farm. For that, bacterium was isolated from three different poultry farm in and around Bangladesh Agricultural University campus for obtaining antibiotic resistance bacteria. Considering the availability and Grams staining properties, *Bacillus* spp. and *Pseudomonas* spp. were selected as potential candidate of Gram-positive and Gram-negative species, respectively. Isolation and identification of bacteria were performed using cultural, gram staining, sugar fermentation, and genius specific PCR investigation [80, 117]. For isolating *Bacillus* spp. and *Pseudomonas* spp., blood agar (BA) and MacConkey agar (MCA) were used as selective media [78, 118]. In BA medium, colonies were arranged as large, flat, and granular to ground-glass with β-hemolysis [119]. The β-hemolysis appeared due to the presence of hemolysin enzyme that completely break down the blood cell and displayed clear halos around bacterial colony suggesting growth of *Bacillus* spp. [120]. In case of MCA medium, circular, smooth, raised, and blue-green colonies indicating growth of *Pseudomonas* spp. [119]. Likewise, microscopic investigations revealed purple color and rod-shaped with square ended bacteria in stained smear prepared from BA confirming Gram-positive *Bacillus* spp. [117, 121]. While, staining from MCA revealed small rod with pink color bacteria confirmed Gram-negative *Pseudomonas* spp. [122]. Additionally, sugar fermentation test was also employed for further confirmation of isolates by observing changes of color and production of gases. Isolates from BA exhibited no color change (pinkish) for all the four basic sugar in comparison with control, while dextrose turned to orange color without gas formation in Durham's tube suggesting presence of *Bacillus* spp. [123]. Whereas, no color change (pinkish) for all the four basic sugars without production of gases were exhibited, while the color of mannitol sugar was changes from pink to orange without gas production in cases of isolates from MCA suggesting presence of *Pseudomonas* spp. [124]. Furthermore, PCR test for all culturally and morphologically detected isolates were performed with their gene specific primers. Here, *16s rRNA* and *16s rDNA* primers were used for amplifying the DNA templates obtained from the isolates of BA and MCA, respectively [125, 126]. The amplicon of 463 bp and 618 bp on gel documentation confirmed the presence of *Bacillus* spp. and *Pseudomonas* spp., respectively [80, 81].

The PCR confirmed bacterial species were subjected to determination of antibiotic resistance pattern phenotypically using 12 commercial antibiotics from different classes and groups such as gentamycin, ampicillin, cefixime, aztreonam, vancomycin, doxycycline, linezolid, erythromycin, chloramphenicol, trimethoprim, levofloxacin, and moxifloxacin following the disc diffusion methods [127]. *Bacillus* spp. was resistant to 10 antibiotics and *Pseudomonas* spp. was resistant to 11 antibiotics indicating both the isolates were multidrug resistance (MDR). It is well known that the isolates that are resistant to more than three antibiotics class are known as MDR [128–132]. Using those MDR isolates, the antibacterial effect of Ag-NPs was verified in comparison with commercial antibiotics. Here, the zone of inhibition of $\leq$15 mm for various antibiotics was known to be resistant according to CLSI, 2019 [133]. Even though both *Bacillus* spp. and *Pseudomonas* spp. showed resistance to cephalexin and chloramphenicol, the Ag-NPs produces sensitive zone of inhibition against them. Herein, Ag-NPs showed inhibitory zone diameter ˃15 mm for all the cases suggesting that Ag-NPs were an effective alternative of antibiotics. The stability assay of Ag-NPs revealed that the yielded solutions were stable till 5^{th} day post synthesis because of their agglomeration tendency after prolog periods of post synthesis. Therefore, to achieve stability for prolong periods the yielded particle needs to be lyophilized [134]. The minimum inhibitory concentration (MIC) of Ag-NPs for inhibiting bacterial growth was measured based on transmittance spectra obtained from UV-Vis spectroscopy [84, 85, 135]. The turbidity of the broth due to bacterial growth showed a reciprocal relationship with the transmittance value, while transmittance ranges from 100 to 96% utilized as an indicator for bacterial growth inhibition as mentioned elsewhere [136]. Such spectroscopic observations were employed for determining MIC of newly synthesized Ag-NPs. The MIC value of synthesized Ag-NPs was 1.06 μg/ml for *Bacillus* spp. and 4.2 μg/ml for *Pseudomonas* spp., indicating that 4.2 μg/ml of Ag-NPs can completely inhibit the growth of both the Gram-positive and Gram-negative bacteria [85, 86, 136]. Likewise, the minimum bacterial concentration (MBC) was also determined, following the agar dilution methods [86]. The MBC of Ag-NPs 2.1 μg/ml for Gram-positive and 8.5 μg/ml for Gram-negative reveals that 8.5 μg/ml of Ag-NPs can kill 10^5 CFU/ml of antibiotic resistance bacterial. Both the MIC and MBC value revealed that the newly synthesized Ag-NPs inhibit bacterial growth at ten times less concentration of Ag-NPs compared to previously synthesized Ag-NPs (Table S1). This significant enhancement of newly synthesized Ag-NPs is due to the availability of positively charged surface area since the particle was synthesized without a capping agent. Such noncapped positively charged Ag-NPs electrostatically interacted with the negatively charged bacterial cell wall for exerting the antibacterial effect [7]. Thus, the synthesized Ag-NPs with excellent antimicrobial activity against both the Gram-positive and Gram-negative bacteria hold a promise to be an effective alternative to commercial antibiotics in controlling resistant microflora in the farm environment as well as to prevent the spreading resistance gene among other environmental flora through plasmid shearing.

The biosafety compliance of any therapeutics is considered as major steps prior to their *in vivo* applications [137]. Considering this, the present study evaluates biosafety of the synthesized Ag-NPs on BHK-21 cell line by measuring cell viability using a trypen blue exclusion assay [138, 139]. This trypen blue-based cell viability data showed a nonsignificant difference in between the control and $\geq$2 MIC doses Ag-NPs treatment. Whereas, the significant difference in the cell viability was observed from cells treated with 3 MIC dose. In case of 3 MIC dose, the cell viability was decreased due to the changes of pH of the cell culture media. Usually, *in vitro* cell culture 7.4 pH is critically required whereas, 3 MIC dose of Ag-NPs solution breaks this pH homeostasis because of the presence of STPP [140–142]. This study employed Ag-NPs solution containing unused STPP which may be responsible for such decrease in cell viability. However, lyophilized Ag-NPs from the yielded solution could overcome this pH change-based decrease in cell viability. Such lyophilized Ag-NPs would be safe even at several-fold higher MIC doses.

5. Conclusions

This facile synthesis programme successfully synthesized Ag-NPs employing silver nitrate ($AgNO_3$) as the ion source and sodium tripolyphosphate (STPP) as reducing as well as capping agents. The homogenously distributed, round shaped, and 100–300 nm size Ag-NPs was revealed from 0.01 M ion source after 4 h reduction reaction with 1% STPP. The synthesized Ag-NPs showed excellent sensitivity against MDR positive *Bacillus* spp. and *Pseudomonas* spp. isolated from poultry farm environment. The particles concentration and antibacterial effect was stable up to 5 (five) days post synthesis in their aqueous state. The particle showed excellent broad-spectrum activity against both Gram-positive and Gram-negative bacteria. The yielded Ag-NPs were nontoxic for the living system up to 2 MIC doses. Thus, the synthesized Ag-NPs could be an effective alternative of antibiotics for tackling bacterial infection in poultry farm. Such application of antibacterial Ag-NPs will carve the use of antibiotics in poultry farming.

Data Availability

The data used to support the findings of this study are available from the corresponding author upon request.

Conflicts of Interest

The authors declare that they have no conflicts of interest.

Acknowledgments

The authors acknowledge all laboratory staffs of the department of Microbiology and Hygiene, BAU. The Bangladesh Agricultural University Research System (BAURES, Project. no. 2021/81/BAU) funded this research.

Supplementary Materials

Figures S1a–S1b show biochemical characterization of *Pseudomonas* spp. and *Bacillus* spp., and Table S1 showsthe comparative analysis of Ag-NPs synthesis with previously synthesized antibacterial Ag-NPs. (*Supplementary Materials*)

References

[1] D. W. Nelson, J. E. Moore, and J. R. Rao, "Antimicrobial resistance (AMR): significance to food quality and safety," *Food Quality and Safety*, vol. 3, no. 1, pp. 15–22, 2019.

[2] A. I. Samreen, I. Ahmad, H. A. Malak, and H. H. Abulreesh, "Environmental antimicrobial resistance and its drivers: a potential threat to public health," *Journal of Global Antimicrobial Resistance*, vol. 27, pp. 101–111, 2021.

[3] M. Z. Hosain, S. M. L. Kabir, and M. M. Kamal, "Antimicrobial uses for livestock production in developing countries," *Veterinary World*, vol. 14, no. 1, pp. 210–221, 2021.

[4] M. H. Haque, S. Sarker, M. S. Islam et al., "Sustainable antibiotic-free broiler meat production: current trends, challenges, and possibilities in a developing country perspective," *Biology*, vol. 9, no. 11, p. 411, 2020.

[5] L. Pokludová, "Antimicrobials in livestock 1: regulation, science, practice. Antimicrob. Livest. 1," *Regul. Sci. Pract*, Springer, Cham, Switzerland, 2020.

[6] M. de Mesquita Souza Saraiva, K. Lim, D. F. M. do Monte, P. E. N. Givisiez, L. B. R. Alves, and O. C. de Freitas Neto, *Antimicrobial Resistance in the Globalized Food Chain: A One Health Perspective Applied to the Poultry Industry. Brazilian J Microbiol*, Springer International Publishing, Berlin, Germany, 2021.

[7] W. Gao and L. Zhang, "Nanomaterials arising amid antibiotic resistance," *Nature Reviews Microbiology*, vol. 19, no. 1, pp. 5-6, 2021.

[8] L. Serwecinska, "Antimicrobials and antibiotic-resistant bacteria," *Water*, vol. 12, pp. 1–17, 2020.

[9] M. A. R. Al Azad, M. M. Rahman, R. Amin et al., "Susceptibility and multidrug resistance patterns of Escherichia coli isolated from cloacal swabs of live broiler chickens in Bangladesh," *Pathogens*, vol. 8, pp. 1–9, 2019.

[10] I. Ahmed, M. B. Rabbi, and S. Sultana, "Antibiotic resistance in Bangladesh: a systematic review," *International Journal of Infectious Diseases*, vol. 80, pp. 54–61, 2019.

[11] M. Rizwan and M. Naeem, "Isolation & Identification of Shigella species from food and water samples of Quetta, Pakistan," *Pure Appl Biol*, vol. 7, 2018.

[12] M. Fernández, S. Conde, J. De La Torre, C. Molina-Santiago, J. L. Ramos, and E. Duque, "Mechanisms of resistance to chloramphenicol in Pseudomonas putida KT2440," *Antimicrobial Agents and Chemotherapy*, vol. 56, no. 2, pp. 1001–1009, 2012.

[13] M. K. Karamoddini, B. S. Fazli-Bazzaz, F. Emamipour et al., "Antibacterial efficacy of lytic bacteriophages against antibiotic-resistant Klebsiella species," *The Scientific World Journal*, vol. 11, pp. 1332–1340, 2011.

[14] M. Kotakonda, S. Valiyaparambil, S. T. Benson, D. Venkatachalam, and V. K. Ravindran, "Phenotypic characterization of antimicrobial resistance in Kerala Bacillus spp isolated from paddy field," vol. 2, pp. 75–78, 2017.

[15] M. Rani Sarkar, M. H. Rashid, A. Rahman et al., "Recent advances in nanomaterials based sustainable agriculture: an overview," *Environmental Nanotechnology, Monitoring & Management*, vol. 18, Article ID 100687, 2022.

[16] E. P. Lesho and M. Laguio-Vila, "The slow-motion catastrophe of antimicrobial resistance and practical interventions for all prescribers," *Mayo Clin Proc [Internet]*,Mayo Foundation for Medical Education and Research, vol. 94, pp. 1040–1047, 2019.

[17] D. R. Dodds, "Antibiotic resistance: A current epilogue," *Biochem Pharmacol. Elsevier Inc*, vol. 134, pp. 139–146, 2017.

[18] L. A. D. R. Minarini, L. N. Andrade, E. De Gregorio et al., "Editorial: antimicrobial resistance as a global public health problem: how can we address it?" *Frontiers in Public Health*, vol. 8, pp. 1–6, 2020.

[19] C. Hernández-Quevedo and B. Rechel, "The role of public health organizations in addressing obesity in Europe," *The European Journal of Public Health*, vol. 28, 2018.

[20] P. Prosposito, F. Mochi, E. Ciotta et al., "Hydrophilic silver nanoparticles with tunable optical properties: application for the detection of heavy metals in water," *Beilstein Journal of Nanotechnology*, vol. 7, pp. 1654–1661, 2016.

[21] X. F. Zhang, Z. G. Liu, W. Shen, and S. Gurunathan, "Silver nanoparticles: synthesis, characterization, properties, applications, and therapeutic approaches," *International Journal of Molecular Sciences*, vol. 17, no. 9, p. 1534, 2016.

[22] M. Godoy-Gallardo, U. Eckhard, L. M. Delgado et al., "Antibacterial approaches in tissue engineering using metal ions and nanoparticles: from mechanisms to applications," *Bioactive Materials*, vol. 6, no. 12, pp. 4470–4490, 2021.

[23] A. Vassallo, M. F. Silletti, I. Faraone, and L. Milella, "Nanoparticulate antibiotic systems as antibacterial agents and antibiotic delivery platforms to fight infections," *Journal of Nanomaterials*, vol. 2020, Article ID 6905631, 31 pages, 2020.

[24] F. Torabian, A. Akhavan Rezayat, M. Ghasemi Nour, A. Ghorbanzadeh, S. Najafi, and A. Sahebkar, "Administration of Silver Nanoparticles in Diabetes Mellitus: A Systematic Review and Meta-analysis on Animal Studies," *Biol Trace Elem Res. Springer US*, vol. 200, pp. 1699–1709, 2022.

[25] N. Khandan Nasab, Z. Sabouri, S. Ghazal, and M. Darroudi, "Green-Based Synthesis of Mixed-phase Silver Nanoparticles as an Effective Photocatalyst and Investigation of Their Antibacterial Properties," *J Mol Struct. Elsevier B.V*, vol. 1203, 2020.

[26] Z. Sabouri, M. Sabouri, M. S. Amiri, M. Khatami, and M. Darroudi, "Plant-based synthesis of cerium oxide nanoparticles using Rheum turkestanicum extract and evaluation of their cytotoxicity and photocatalytic properties," *Materials Technology*, vol. 37, no. 8, pp. 555–568, 2022.

[27] Z. Sabouri and S. Sabouri, S. S. Hafez Moghaddas, A. Mostafapour, M. S. Amiri, and M. Darroudi, Facile green synthesis of Ag-doped ZnO/CaO nanocomposites with Caccinia macranthera seed extract and assessment of their cytotoxicity, antibacterial, and photocatalytic activity," *Bioprocess Biosyst Eng. Springer Berlin Heidelberg*, vol. 45, pp. 1799–1809, 2022.

[28] M. E. T. Yazdi, M. Darroudi, M. S. Amiri et al., "Anticancer, antimicrobial, and dye degradation activity of biosynthesised silver nanoparticle using Artemisia kopetdaghensis," *Micro & Nano Letters*, vol. 15, pp. 1065–1070, 2020.

[29] M. A. Kafi, H. Y. Cho, and J. W. Choi, "Neural cell chip based electrochemical detection of nanotoxicity," *Nanomaterials*, vol. 5, no. 3, pp. 1181–1199, 2015.

[30] N. Jain, P. Jain, D. Rajput, and U. K. Patil, "Green synthesized plant-based silver nanoparticles: therapeutic prospective for anticancer and antiviral activity," *Micro Nano Syst Lett. Springer Singapore*, vol. 9, 2021.

[31] Z. Yang, S. He, H. Wu, T. Yin, L. Wang, and A. Shan, "Nanostructured antimicrobial peptides: crucial steps of

overcoming the bottleneck for clinics," *Frontiers in Microbiology*, vol. 12, pp. 1–28, 2021.

[32] Z. Sabouri, S. Sabouri, S. S. T. H. Moghaddas, A. Mostafapour, S. M. Gheibihayat, and M. Darroudi, *Plant-based Synthesis of Ag-Doped ZnO/MgO Nanocomposites Using Caccinia Macranthera Extract and Evaluation of Their Photocatalytic Activity*,Cytotoxicity, and Potential Application as a Novel Sensor for Detection of Pb2+ Ions. Biomass Convers Biorefinery, Springer Berlin Heidelberg, Berlin, Germany, 2022.

[33] M. A. Kafi, T. H. Kim, T. Lee, and J. W. Choi, "Cell chip with nano-scale peptide layer to detect dopamine secretion from neuronal cells," *Journal of Nanoscience and Nanotechnology*, vol. 11, no. 8, pp. 7086–7090, 2011.

[34] A. Vilouras, A. Paul, M. A. Kafi, and R. Dahiya, "Graphene oxide-chitosan based ultra-flexible electrochemical sensor for detection of serotonin," *Proc IEEE Sensors. IEEE*, 2018.

[35] M. A. Kafi, H. Y. Cho, and J. W. Choi, "Engineered peptide-based nanobiomaterials for electrochemical cell chip," *Nano Convergence*, vol. 3, no. 1, p. 17, 2016.

[36] M. A. Kafi, A. Paul, A. Vilouras, E. S. Hosseini, and R. S. Dahiya, "Chitosan-Graphene Oxide-Based Ultra-thin and Flexible Sensor for Diabetic Wound Monitoring," in *Proceedings of the IEEE Sens J. Institute of Electrical and Electronics Engineers Inc*, pp. 6794–6801, New Delhi, India, October 2018.

[37] O. Hossain, E. Rahman, H. Roy, M. S. Azam, and S. Ahmed, "Synthesis, characterization, and comparative assessment of antimicrobial properties and cytotoxicity of graphene-, silver-, and zinc-based nanomaterials," *Analytical Science Advances*, vol. 3, no. 1-2, pp. 54–63, 2022.

[38] Y. Wang, Q. M. Wang, W. Feng et al., "Antibacterial activity and mechanism of moxifloxacin nanoparticles against drug-resistant Pseudomonas aeruginosa," *Yaoxue Xuebao*, vol. 55, pp. 2460–2465, 2020.

[39] K. J. Roy, A. Rahman, K. Hossain, and B. Rahman, "Antibacterial investigation of silver nanoparticle against Staphylococcus, E. coli and Salmonella isolated from selected live bird markets," *Appl Microbiol Open Access*, vol. 6, p. 173, 2020.

[40] D. Sharma, S. Kanchi, and K. Bisetty, "Biogenic synthesis of nanoparticles: a review," *Arabian Journal of Chemistry*, vol. 12, no. 8, pp. 3576–3600, 2019.

[41] A. Tavakoli, M. Sohrabi, and A. Kargari, "A review of methods for synthesis of nanostructured metals with emphasis on iron compounds," *Chemical Papers*, vol. 61, no. 3, pp. 151–170, 2007.

[42] L. Nejdl, J. Zitka, F. Mravec et al., "Real-time monitoring of the UV-induced formation of quantum dots on a milliliter, microliter, and nanoliter scale," *Microchimica Acta*, vol. 184, no. 5, pp. 1489–1497, 2017.

[43] K. Okuyama and I. Wuled Lenggoro, "Preparation of nanoparticles via spray route," *Chemical Engineering Science*, vol. 58, no. 3-6, pp. 537–547, 2003.

[44] R. Suciu, I. Kantor, H. Bütün, and F. Maréchal, "Geographically parameterized residential sector energy and service profile," *Frontiers in Energy Research*, vol. 7, pp. 1–19, 2019.

[45] P. Govindrao, N. W. Ghule, A. Haque, and M. G. Kalaskar, "Journal of Drug Delivery Science and Technology Metal nanoparticles synthesis: An overview on methods of preparation, advantages and disadvantages, and applications," *J Drug Deliv Sci Technol. Elsevier*, vol. 53, Article ID 101174, 2019.

[46] K. W. Shah, G. F. Huseien, and H. W. Kua, "A state-of-the-art review on core–shell pigments nanostructure preparation and test methods," *Micro*, vol. 1, pp. 55–85, 2021.

[47] R. Javed, M. Zia, S. Naz, S. O. Aisida, N. Ain, and Q. Ao, "Role of capping agents in the application of nanoparticles in biomedicine and environmental remediation: recent trends and future prospects," *Journal of Nanobiotechnology*, vol. 18, pp. 1–15, 2020.

[48] G. Habibullah, J. Viktorova, and T. Ruml, "Current strategies for noble metal nanoparticle synthesis," *Nanoscale Research Letters*, vol. 16, no. 1, p. 47, 2021.

[49] R. Indiarto, L. P. A. Indriana, R. Andoyo, E. Subroto, and B. Nurhadi, "Bottom–up nanoparticle synthesis: a review of techniques, polyphenol-based core materials, and their properties," *European Food Research and Technology*. Springer Berlin Heidelberg, vol. 248, pp. 1–24, 2022

[50] N. M. Noah, "Design and synthesis of nanostructured materials for sensor applications," *Journal of Nanomaterials*, vol. 2020, pp. 1–20, 2020.

[51] R. A. Hamouda, M. H. Hussein, R. A. Abo-elmagd, and S. S. Bawazir, "Synthesis and biological characterization of silver nanoparticles derived from the cyanobacterium Oscillatoria limnetica," *Scientific Reports*, vol. 9, pp. 1–17, 2019.

[52] I. Wiegand, K. Hilpert, and R. E. W. Hancock, "Agar and broth dilution methods to determine the minimal inhibitory concentration (MIC) of antimicrobial substances," *Nature Protocols*, vol. 3, no. 2, pp. 163–175, 2008.

[53] C. Rodríguez-Melcón, C. Alonso-calleja, C. García-Fernández, J. Carballo, and R. Capita, "Minimum inhibitory concentration (MIC) and minimum bactericidal concentration (MBC) for twelve antimicrobials (biocides and antibiotics) in eight strains of Listeria monocytogenes," *Biology*, vol. 11, no. 1, p. 46, 2021.

[54] A. Saadat, A. Dehghani Varniab, and S. M. Madani, "Prediction of the antibacterial activity of the green synthesized silver nanoparticles against gram negative and positive bacteria by using machine learning algorithms," *Journal of Nanomaterials*, vol. 2022, Article ID 4986826, 10 pages, 2022.

[55] L. Huang, H. Yang, Y. Zhang, and W. Xiao, "Study on synthesis and antibacterial properties of Ag NPs/GO nanocomposites," *Journal of Nanomaterials*, vol. 2016, Article ID 5685967, 9 pages, 2016.

[56] M. M. Hassan, M. E. El Zowalaty, A. Lundkvist et al., "Residual antimicrobial agents in food originating from animals," *Trends in Food Science & Technology*, vol. 111, pp. 141–150, 2021.

[57] C. Agyare, V. Etsiapa Boamah, C. Ngofi Zumbi, and F. Boateng Osei, *Antibiotic Use in Poultry Production and its Effects on Bacterial Resistance*, Antimicrob Resist - A Glob Threat, 5 Princes Gate Court, London, UK, 2019.

[58] L. A. Selaledi, Z. M. Hassan, T. G. Manyelo, and M. Mabelebele, "The current status of the alternative use to antibiotics in poultry production: an African perspective," *Antibiotics*, vol. 9, pp. 1–18, 2020.

[59] S. Najoom, F. Fozia, I. Ahmad et al., "Effective antiplasmodial and cytotoxic activities of synthesized zinc oxide nanoparticles using rhazya stricta leaf extract," *Evidence-based Complementary and Alternative Medicine*, vol. 2021, Article ID 5586740, pp. 2021–2029, 2021.

[60] W. Szczepanik, P. Kaczmarek, and M. Jezowska-Bojczuk, "Oxidative activity of copper (II) complexes with aminoglycoside antibiotics as implication to the toxicity of these

drugs," *Bioinorganic Chemistry and Applications*, vol. 2, no. 1-2, pp. 55–68, 2004.

[61] G. Tao, L. Liu, Y. Wang et al., "Characterization of silver nanoparticle in situ synthesis on porous sericin gel for antibacterial application," *Journal of Nanomaterials*, vol. 2016, Article ID 9505704, 8 pages, 2016.

[62] A. A. Pawar, J. Sahoo, A. Verma et al., "Azadirachta indica -derived silver nanoparticle synthesis and its antimicrobial applications," *Journal of Nanomaterials*, vol. 2022, Article ID 4251229, 15 pages, 2022.

[63] A. Yildiz and M. Değirmencioğlu, "Synthesis of silver abietate as an antibacterial agent for textile applications," *Bioinorganic Chemistry and Applications*, vol. 2015, Article ID 215354, 5 pages, 2015.

[64] D. G. Larrude, M. E. H. Maia Da Costa, and F. L. Freire, "Synthesis and characterization of silver nanoparticle-multiwalled carbon nanotube composites," *Journal of Nanomaterials*, vol. 2014, Article ID 654068, 7 pages, 2014.

[65] Y. Jeong, D. W. Lim, and J. Choi, "Assessment of size-dependent antimicrobial and cytotoxic properties of silver nanoparticles," *Advances in Materials Science and Engineering*, vol. 2014, Article ID 763807, 6 pages, 2014.

[66] S. Rao, C. Huang, U. Tata et al., "Evaluation of cytotoxic effects of different concentrations of porous Hollow Au Nanoparticles (PHAuNPs) on cells," *Journal of Nanotechnology*, vol. 2014, Article ID 631248, 7 pages, 2014.

[67] F. Namvar, H. S. Rahman, R. Mohamad et al., "Cytotoxic effects of biosynthesized zinc oxide nanoparticles on murine cell lines," *Evidence-based Complementary and Alternative Medicine*, vol. 2015, Article ID 593014, 11 pages, 2015.

[68] W. Khan, N. Khan, N. Jamila et al., "Antioxidant, antibacterial, and catalytic performance of biosynthesized silver nanoparticles of Rhus javanica, Rumex hastatus, and Callistemon viminalis," *Saudi Journal of Biological Sciences*, vol. 29, no. 2, pp. 894–904, 2022.

[69] S. S. Abdulsahib, "Synthesis, characterization and biomedical applications of silver nanoparticles," *Biomedicine*, vol. 41, no. 2, pp. 458–464, 2021.

[70] Y. Sun, A. Bhattacharjee, M. Reynolds, and Y. V. Li, "Synthesis and characterizations of gentamicin loaded polylactic coglycolic (PLGA) nanoparticles," *Journal of Nanoparticle Research*, vol. 23, no. 8, pp. 1–15, 2021.

[71] E. A. Fouad, A. S. M. Abu Elnaga, and M. M. Kandil, "Antibacterial efficacy of Moringa oleifera leaf extract against pyogenic bacteria isolated from a dromedary camel (Camelus dromedarius) abscess," *Veterinary World*, vol. 12, no. 6, pp. 802–808, 2019.

[72] A. Zielińska, E. Skwarek, A. Zaleska, M. Gazda, and J. Hupka, "Preparation of silver nanoparticles with controlled particle size," *Procedia Chemistry*, vol. 1, no. 2, pp. 1560–1566, 2009.

[73] A. Rahman, K. J. Roy, K. M. A. Rahman et al., "Adhesion and proliferation of living cell on surface functionalized with glycine nanostructures," *Nano Select*, vol. 3, pp. 188–200, 2021.

[74] H. A. Ghetas, N. Abdel-Razek, M. S. Shakweer et al., "Antimicrobial activity of chemically and biologically synthesized silver nanoparticles against some fish pathogens," *Saudi Journal of Biological Sciences*, vol. 29, no. 3, pp. 1298–1305, 2022.

[75] A. V. Maduka, C. O. Samuel, O. O. Oluwatoyin, O. J. Orji, and C. E. Elsie, "Microbiological analysis of outdoor air quality of male and female hostels in ebonyi state university," *Abakaliki , Ebonyi*.vol. 11, pp. 68–73, 2016.

[76] A. L. Tariq, S. Sudha, and A. L. Reyaz, "Isolation and screening of Bacillus species from sediments and application in bioremediation," *International Journal of Current Microbiology and Applied Sciences*, vol. 5, no. 6, pp. 916–924, 2016.

[77] F. A. Al-Dhabaan, "Morphological, biochemical and molecular identification of petroleum hydrocarbons biodegradation bacteria isolated from oil polluted soil in Dhahran, Saud Arabia," *Saudi Journal of Biological Sciences*, vol. 26, no. 6, pp. 1247–1252, 2019.

[78] M. Y. Al-Hejjaj, S. S. Al-Amara, Y. A. Dawood, S. J. Raisan, and H. M. Al-Tameemi, "Molecular detection of new bacillus strains from soil samples of free grazing areas in Basrah Province, Southern Iraq," *Annals of Tropical Medicine and Public Health*, vol. 23, no. 11, 2020.

[79] R. Ali El Hadi Mohamed, D. M. Abdelgadir, H. M. Bashab et al., "First record of West Nile Virus detection inside wild mosquitoes in Khartoum capital of Sudan using PCR," *Saudi Journal of Biological Sciences*, vol. 27, no. 12, pp. 3359–3364, 2020, https://doi.org/10.1016/j.sjbs.2020.08.047.

[80] S. Kadyan, M. Panghal, K. Singh, and J. P. Yadav, "Development of a PCR based marker system for easy identification and classification of aerobic endospore forming Bacilli," *SpringerPlus*, vol. 2, pp. 1–19, 2013.

[81] T. Spilker, T. Coenye, P. Vandamme, and J. J. LiPuma, "PCR-based assay for differentiation of Pseudomonas aeruginosa from other Pseudomonas species recovered from cystic fibrosis patients," *Journal of Clinical Microbiology*, vol. 42, no. 5, pp. 2074–2079, 2004.

[82] B. Limbago, "M100-S11, Performance standards for antimicrobial susceptibility testing," *Clinical Microbiology Newsletter*, vol. 23, p. 49, 2001.

[83] M. Balouiri, M. Sadiki, and S. K. Ibnsouda, "Methods for in vitro evaluating antimicrobial activity: A review," *J Pharm Anal. Elsevier*, vol. 6, pp. 71–79, 2016.

[84] A. Manuel and N. Abdulrahman, "Determination of minimum inhibitory concentration of liposomes: a novel method," *International Journal of Current Microbiology and Applied Sciences*, vol. 6, no. 8, pp. 1140–1147, 2017.

[85] M. B. Binish, P. Binu, V. G. Gopikrishna, and M. Mohan, *Potential of Anaerobic Bacteria in Bioremediation of Metal-Contaminated marine and Estuarine Environment*, Microb. Biodegrad. Bioremediation. INC, Amsterdam, Netherlands, 2022.

[86] B. Kowalska-Krochmal and R. Dudek-Wicher, "The minimum inhibitory concentration of antibiotics: methods, interpretation, clinical relevance," *Pathogens*, vol. 10, no. 2, pp. 1–21, 2021.

[87] D. U. Kim, J. W. Han, S. J. Jung et al., "Comparison of alcian blue, trypan blue, and toluidine blue for visualization of the primo vascular system floating in lymph ducts," *Evidence-based Complementary and Alternative Medicine*, vol. 2015, Article ID 725989, 8 pages, 2015.

[88] J. H. Lim, J. E. Lee, C. J. Park, and J. B. Park, "Evaluation of the effects of mouthwash on the morphology and cell viability of osteoblast-like cells," *BioMed Research International*, vol. 2022, Article ID 5884974, 6 pages, 2022.

[89] S. Kamiloglu, G. Sari, T. Ozdal, and E. Capanoglu, "Guidelines for cell viability assays," *Food Frontiers*, vol. 1, no. 3, pp. 332–349, 2020.

[90] C. Cheng, C. Liu, B. Han et al., "Silver nanoparticles modified with sodium triphosphate: antibacterial activity, hemocompatibility and cytotoxicity," *Journal of Nanoscience and Nanotechnology*, vol. 18, no. 6, pp. 3816–3824, 2018.

[91] P. Selvakumar, R. Sithara, K. Viveka, and P. Sivashanmugam, "Green synthesis of silver nanoparticles using leaf extract of Acalypha hispida and its application in blood compatibility," *Journal of Photochemistry and Photobiology B: Biology*, vol. 182, pp. 52–61, 2018.

[92] H. Peng, Y. Liu, W. Peng, J. Zhang, and R. Ruan, "Green synthesis and stability evaluation of Ag nanoparticles using bamboo hemicellulose," *Bioresources*, vol. 11, pp. 385–399, 2016.

[93] M. Chakravarty and A. Vora, "Nanotechnology-based antiviral therapeutics," *Drug Delivery and Translational Research*, vol. 11, no. 3, pp. 748–787, 2021.

[94] S. Y. Oh, N. S. Heo, S. Shukla et al., "Development of gold nanoparticle-aptamer-based LSPR sensing chips for the rapid detection of Salmonella typhimurium in pork meat," *Scientific Reports*, vol. 7, pp. 1–21, 2017.

[95] R. La Spina, D. Mehn, F. Fumagalli et al., "Synthesis of citrate-stabilized silver nanoparticles modified by thermal and ph preconditioned tannic acid," *Nanomaterials*, vol. 10, pp. 1–16, 2020.

[96] M. Wang, H. Li, Y. Li et al., "Dispersibility and size control of silver nanoparticles with anti-algal potential based on coupling effects of polyvinylpyrrolidone and sodium tripolyphosphate," *Nanomaterials*, vol. 10, no. 6, p. 1042, 2020.

[97] M. E. Di Ianni, G. A. Islan, C. Y. Chain, G. R. Castro, A. Talevi, and M. E. Vela, "Interaction of solid lipid nanoparticles and specific proteins of the corona studied by surface plasmon resonance," *Journal of Nanomaterials*, vol. 2017, Article ID 6509184, 11 pages, 2017.

[98] T. Hira, T. Uchiyama, K. Kuwamura, Y. Kihara, T. Yawatari, and T. Saiki, "Switching the localized surface plasmon resonance of single gold nanorods with a phase-change material and the implementation of a cellular automata algorithm using a plasmon particle array," *Advances in Optical Technologies*, vol. 2015, Article ID 150791, 5 pages, 2015.

[99] G. Arroyo, Y. Angulo, A. Debut, and L. H. Cumbal, "Synthesis and characterization of silver nanoparticles prepared with carrasquilla fruit extract (Berberis hallii) and evaluation of its photocatalytic activity," *Catalysts*, vol. 11, no. 10, p. 1195, 2021.

[100] S. Dawadi, S. Katuwal, A. Gupta et al., "Current research on silver nanoparticles: synthesis, characterization, and applications," *Journal of Nanomaterials*, vol. 2021, Article ID 6687290, pp. 2021–23, 2021.

[101] T. Wang and N. He, "Preparation, characterization and applications of low molecular weight alginate oligochitosan nanocapsules," *Nanoscale*, vol. 2, pp. 230–239, 2010.

[102] S. A. Fincer, P. Fertilizers, A. J. Klanica, and T. F. Korenowski,, "Process for making sodium tripolyphosphate from wet process phosphoric acid," *Patent no. US4251491A*,no. 19, pp. 4–9, 1981.

[103] J. García-Barrasa, J. M. López-De-luzuriaga, and M. Monge, "Silver nanoparticles: synthesis through chemical methods in solution and biomedical applications," *Open Chemistry*, vol. 9, no. 1, pp. 7–19, 2011.

[104] Z. Wei, G. Jacquemod, Y. Leduc, E. Foucauld, J. Prouvee, and B. Blampey, "Reducing the short channel effect of transistors and reducing the size of analog circuits," *Act Passiv Electron Components*, vol. 2019, Article ID 4578501, 9 pages, 2019.

[105] O. Rojviroon, S. Sirivithayapakorn, T. Rojviroon, and C. Wantawin, "Effects of initial nitrate concentrations and photocatalyst dosages on ammonium ion in synthetic wastewater treated by photocatalytic reduction," *International Journal of Photoenergy*, vol. 2020, Article ID 8893816, 9 pages, 2020.

[106] P. Bélteky, A. Rónavári, N. Igaz et al., *International Journal of Nanomedicine*, vol. 14, pp. 667–687, 2019.

[107] L. M. Fu, J. H. Hsu, M. K. Shih et al., "Process optimization of silver nanoparticle synthesis and its application in mercury detection," *Micromachines*, vol. 12, no. 9, pp. 1–16, 2021.

[108] F. A. Al-Marhaby and R. Seoudi, "Preparation and characterization of silver nanoparticles and their use in catalytic reduction of 4-nitrophenol," *World Journal of Nano Science and Engineering*, vol. 06, no. 01, pp. 29–37, 2016.

[109] O. M. Bello, O. S. Oguntoye, A. O. Dada et al., "Phytobiological-facilitated production of silver nanoparticles from selected non-cultivated vegetables in Nigeria and their biological potential," *Turkish Journal of Pharmaceutical Sciences*, vol. 17, no. 6, pp. 599–609, 2020.

[110] B. Guven, M. Eryilmaz, A. Üzer, I. H. Boyaci, U. Tamer, and R. Apak, "Surface-enhanced Raman spectroscopy combined with gold nanorods for the simultaneous quantification of nitramine energetic materials," *RSC Advances*, vol. 7, no. 59, pp. 37039–37047, 2017.

[111] P. Rauwel, S. Küünal, S. Ferdov, and E. Rauwel, "A review on the green synthesis of silver nanoparticles and their morphologies studied via TEM," *Advances in Materials Science and Engineering*, vol. 2015, Article ID 682749, 9 pages, 2015.

[112] Y. Zhang, H. Lu, D. Yu, and D. Zhao, "AgNPs and Ag/C225 exert anticancerous effects via cell cycle regulation and cytotoxicity enhancement," *Journal of Nanomaterials*, vol. 2017, Article ID 7920368, 10 pages, 2017.

[113] S. Rajeshkumar, "Citrus lemon juice mediated preparation of AgNPs/chitosan-based bionanocomposites and its antimicrobial and antioxidant activity," *Journal of Nanomaterials*, vol. 2021, pp. 1–9, Article ID 7527250, 2021.

[114] A. Noshad, M. Iqbal, C. Hetherington, and H. Wahab, "Biogenic AgNPs - a nano weapon against bacterial canker of tomato (bct)," *Advances in Agriculture*, vol. 2020, Article ID 9630785, 10 pages, 2020.

[115] E. Kovalska, P. K. Roy, N. Antonatos et al., "Photocatalytic activity of twist-angle stacked 2D TaS2. npj 2D Mater Appl," *Npj 2D Materials and Applications*,Springer US, vol. 5, pp. 1–9, 2021.

[116] M. Bin Ahmad, J. J. Lim, K. Shameli, N. A. Ibrahim, and M. Y. Tay, "Synthesis of silver nanoparticles in chitosan, gelatin and chitosan/gelatin bionanocomposites by a chemical reducing agent and their characterization," *Molecules*, vol. 16, no. 9, pp. 7237–7248, 2011.

[117] R. Vazquez-Muñoz, A. Meza-Villezcas, P. G. J. Fournier et al., "Enhancement of antibiotics antimicrobial activity due to the silver nanoparticles impact on the cell membrane," *PLoS One*, vol. 14, no. 11, pp. e0224904–e0224918, 2019.

[118] Y. Xu, F. Y. H. Kutsanedzie, H. Sun et al., "Rapid Pseudomonas species identification from chicken by integrating colorimetric sensors with near-infrared spectroscopy," *Food Analytical Methods*, vol. 11, no. 4, pp. 1199–1208, 2018.

[119] Z. Lu, W. Guo, and C. Liu, *Journal of Veterinary Medical Science*, vol. 80, no. 3, pp. 427–433, 2018.

[120] J. I. Irorita Fugaban, J. E. Vazquez Bucheli, W. H. Holzapfel, and S. D. Todorov, "Bacteriocinogenic bacillus spp. Isolated from Korean fermented cabbage (kimchi) beneficial or hazardous?" *Fermentation*, vol. 7, no. 2, p. 56, 2021.

[121] J. K. H. Faragi, "Isolation and identification of Bacillus subtilus as) probiotic) from intestinal microflora of common carp Cyprinus carpio L," *Iraqi J Vet Med*, vol. 36, no. 0E, pp. 355–361, 2012.

[122] V. S. Vishwe, S. P. Gajbhiye, S. P. Vaidya, and A. S. Chowdhary, "Isolation and characterization of lipolytic Pseudomonas spp. from oil contaminated water samples," *IOSR J Biotechnol Biochem*, vol. 1, pp. 33–36, 2016.

[123] T. Fujita and H. Nishiura, "Environmental drivers of Bacillus-positive blood cultures in a cancer hospital, Sapporo, Japan," *International Journal of Environmental Research and Public Health*, vol. 15, no. 10, p. 2201, 2018.

[124] S. S. Su, K. Z. W. Lae, and H. Ngwe, "Isolation and identification of Pseudomonas aeruginosa from the clinical soil. Isol identif Pseudomonas aeruginosa from," *Clin Soil*, vol. 8, pp. 271–275, 2018, https://www.researchgate.net/publication/335619903.

[125] S. K. Loong, C. S. Khor, F. L. Jafar, and S. AbuBakar, "Utility of 16S rDNA sequencing for identification of rare pathogenic bacteria," *Journal of Clinical Laboratory Analysis*, vol. 30, no. 6, pp. 1056–1060, 2016.

[126] P. Lakshmi, A. Bharadwaj, and R. K. Srivastava, "Molecular detection and identification of bacteria in urine samples of asymptomatic and symptomatic pregnantwomen by 16S rRNA gene sequencing," *Arch Clin Infect Dis*, vol. 15, no. 3, pp. 1–10, 2020.

[127] V. Rajan, G. K. Sivaraman, A. Vijayan, R. Elangovan, A. Prendiville, and T. T. Bachmann, "Genotypes and phenotypes of methicillin-resistant staphylococci isolated from shrimp aquaculture farms," *Environ Microbiol Rep*., vol. 14, no. 3, pp. 391–399, 2022.

[128] A. Yousefi and S. Torkan, "Uropathogenic Escherichia coli in the urine samples of Iranian dogs: antimicrobial resistance pattern and distribution of antibiotic resistance genes," *BioMed Research International*, vol. 2017, Article ID 4180490, 10 pages, 2017.

[129] M. M. Zafer, M. H. Al-Agamy, H. A. El-Mahallawy, M. A. Amin, and M. S. E. D. Ashour, "Antimicrobial resistance pattern and their beta-lactamase encoding genes among Pseudomonas aeruginosa strains isolated from cancer patients," *BioMed Research International*, vol. 2014, Article ID 101635, 8 pages, 2014.

[130] J. Behravan and Z. Rangsaaz, "Detection and characterization of beta-lactam resistance in Bacillus cereus PTCC 1015," *The Scientific World Journal*, vol. 4, pp. 622–627, 2004.

[131] A. Grant, C. G. Gay, and H. S. Lillehoj, "Bacillus spp. as direct-fed microbial antibiotic alternatives to enhance growth, immunity, and gut health in poultry," *Avian Pathology*, vol. 47, no. 4, pp. 339–351, 2018.

[132] K. M. Osman, A. D. Kappell, A. Orabi et al., "Poultry and beef meat as potential seedbeds for antimicrobial resistant enterotoxigenic Bacillus species: a materializing epidemiological and potential severe health hazard," *Scientific Reports. Springer US*, vol. 8, pp. 1–15, 2018.

[133] D. W. Wanja, P. G. Mbuthia, R. M. Waruiru, L. C. Bebora, H. A. Ngowi, and P. N. Nyaga, "Antibiotic and disinfectant susceptibility patterns of bacteria isolated from farmed fish in kirinyaga county, Kenya," *International Journal of Microbiology*, vol. 2020, Article ID 8897338, 8 pages, 2020.

[134] W. Zhang, "Nanoparticle aggregation: principles and modeling," *Advances in Experimental Medicine and Biology*, vol. 811, pp. 19–43, 2014.

[135] M. Chamundeeswari, S. S. L. Sobhana, J. P. Jacob et al., "Preparation, characterization and evaluation of a biopolymeric gold nanocomposite with antimicrobial activity," *Biotechnology and Applied Biochemistry*, vol. 55, no. 1, pp. 29–35, 2010.

[136] M. Gorjanc and M. Šala, "Durable antibacterial and UV protective properties of cellulose fabric functionalized with Ag/TiO2 nanocomposite during dyeing with reactive dyes," *Cellulose*, vol. 23, no. 3, pp. 2199–2209, 2016.

[137] S. Vijayan, K. Divya, and M. S. Jisha, "In vitro anticancer evaluation of chitosan/biogenic silver nanoparticle conjugate on Si Ha and MDA MB cell lines," *Applied Nanoscience*, Springer International Publishing, vol. 10, pp. 715–728, 2020.

[138] F. Piccinini, A. Tesei, C. Arienti, and A. Bevilacqua, "Cell counting and viability assessment of 2D and 3D cell cultures: expected reliability of the trypan blue assay," *Biological Procedures Online*, vol. 19, pp. 8–12, 2017.

[139] W. Strober, "Trypan blue exclusion test of cell viability," *Current Protocols in Immunology*, vol. 111, no. 1, 2015.

[140] L. Potts, C. Phillips, M. Hwang, S. Fulcher, and H. Choi, "Rescue of human corneal epithelial cells after alkaline insult using renalase derived peptide, RP-220," *International Journal of Ophthalmology*, vol. 12, no. 11, pp. 1667–1673, 2019.

[141] M. J. Masarudin, S. M. Cutts, B. J. Evison, D. R. Phillips, and P. J. Pigram, "Factors determining the stability, size distribution, and cellular accumulation of small, monodisperse chitosan nanoparticles as candidate vectors for anticancer drug delivery: application to the passive encapsulation of [14C]-doxorubicin," *Nanotechnology, Science and Applications*, vol. 8, pp. 67–80, 2015.

[142] J. K. Patra, G. Das, L. F. Fraceto et al., "Nano based drug delivery systems: recent developments and future prospects," *Journal of Nanobiotechnology*, vol. 16, pp. 71–33, 2018.